AGU PUBLICATIONS

Paleoceanography

RESEARCH ARTICLE
10.1002/2015PA002801

Key Points:
- North Pacific paleoceanography reconstructed from planktic foram isotopic data
- Habitat and calcification depths of forams vary with seasonal mixed layer depth
- Carbon isotopes of *Globigerina umbilicata* are proxy for past seawater carbonate

Supporting Information:
- Figures S1–S4 captions
- Figure S1
- Figure S2
- Figure S3
- Figure S4

Correspondence to:
H. Asahi and B.-K. Khim,
asahiro@kopri.re.kr;
bkkhim@pusan.ac.kr

Citation:
Asahi, H., Y. Okazaki, M. Ikehara, B.-K. Khim, S.-I. Nam, and K. Takahashi (2015), Seasonal variability of $\delta^{18}O$ and $\delta^{13}C$ of planktic foraminifera in the Bering Sea and central subarctic Pacific during 1990–2000, *Paleoceanography*, *30*, 1328–1346, doi:10.1002/2015PA002801.

Received 11 MAR 2015
Accepted 21 SEP 2015
Accepted article online 25 SEP 2015
Published online 28 OCT 2015

Seasonal variability of $\delta^{18}O$ and $\delta^{13}C$ of planktic foraminifera in the Bering Sea and central subarctic Pacific during 1990–2000

Hirofumi Asahi[1,2], Yusuke Okazaki[3], Minoru Ikehara[4], Boo-Keum Khim[1], Seung-Il Nam[2], and Kozo Takahashi[3,5]

[1]Department of Oceanography and Marine Research Institute, Pusan National University, Busan, Korea, [2]Korea Polar Research Institute, Incheon, Korea, [3]Department of Earth and Planetary Sciences, Graduate School of Sciences, Kyushu University, Fukuoka, Japan, [4]Center for Advanced Marine Core Research, Kochi University, Nankoku, Japan, [5]Hokusei Gakuen University, Sapporo, Japan

Abstract We evaluated a 10 year time series of $\delta^{18}O$ and $\delta^{13}C$ records from three planktic foraminifers (*Neogloboquadrina pachyderma*, *Globigerina umbilicata*, and *Globigerinita glutinata*) in the Bering Sea and central subarctic Pacific with a focus on their responses to environmental changes. Foraminiferal $\delta^{18}O$ followed the equilibrium equation for inorganic calcite, with species-specific equilibrium offsets ranging from nearly zero (−0.02‰ for *N. pachyderma* and −0.01‰ for *G. umbilicata*) to −0.16‰ (*G. glutinata*). Equilibrium offsets in our sediment trap samples were smaller than those from plankton tow studies, implying that foraminiferal $\delta^{18}O$ was modified by encrustation during settling. Habitat/calcification depths varied from 35–55 m (*N. pachyderma* and *G. umbilicata*) or 25–45 m (*G. glutinata*) during warm, stratified seasons to around 100 m during winter, when the mixed layer depth increases. Unlike $\delta^{18}O$, foraminiferal $\delta^{13}C$ showed species-specific responses to environmental changes. We found a dependency of $\delta^{13}C$ in *G. umbilicata* on CO_3^{2-} concentrations in ambient seawater that agreed reasonably well with published laboratory results, suggesting that $\delta^{13}C$ of *G. umbilicata* is subject to vital effects. In contrast, $\delta^{13}C$ of *N. pachyderma* and *G. glutinata* are likely affected by other species-specific biological activities. Seasonal flux patterns reveal that fossil records of *N. pachyderma* and *G. glutinata* represent annual mean conditions, whereas that of *G. umbilicata* most likely indicates those of a specific season. Because none of these three taxa was abundant from December to February, their fossil records likely do not reflect isotope signals from cold seasons.

1. Introduction

Stable oxygen and carbon isotopes of planktic foraminifera ($\delta^{18}O_{Foram}$ and $\delta^{13}C_{Foram}$, respectively) have been widely used for decades as proxies for reconstructing past oceanographic conditions. Such a successful application is based primarily on the equilibria for inorganic calcification [e.g., *O'Neil et al.*, 1969; *Romanek et al.*, 1992; *Kim and O'Neil*, 1997; *McConnaughey et al.*, 1997]. Further calibrations using samples obtained from laboratory cultures, plankton tows, and sediment traps have confirmed the different species-specific or region-specific responses of foraminifera carbon and oxygen chemistry to various environmental conditions [e.g., *Ortiz et al.*, 1996; *Spero et al.*, 1997; *Bemis et al.*, 1998; *King and Howard*, 2004, 2005; *Sagawa et al.*, 2013]. Because of the availability of data, most paleoceanographic studies depend on calibrations from limited regions. There is a strong need for additional calibrations from different oceanic realms for further paleoceanographic interpretations.

One major issue related to studies of $\delta^{18}O_{Foram}$ lies with the wide range of reported offsets to the equilibrium values, known as "equilibrium offsets." For example, the reported equilibrium offsets for the polar planktic foraminifer *Neogloboquadrina pachyderma* and the subtropical to polar foraminifer *Globigerina bulloides* range from −1.0‰ [e.g., *Bauch et al.*, 1997, 2002; *Mortyn and Charles*, 2003] to negligibly different from zero [e.g., *King and Howard*, 2005; *Jonkers et al.*, 2013; *Sagawa et al.*, 2013]. Such diverse equilibrium offsets are thought to be due to (a) the choice of equilibrium equations [*Kuroyanagi et al.*, 2011], (b) modification of *N. pachyderma* oxygen isotopes via encrustation [*Kohfeld et al.*, 1996; *Kozdon et al.*, 2009], (c) a carbonate ion effect (CIE) seen in *G. bulloides* [*Spero et al.*, 1997], and (d) morphologic or genotypic differences in *N. pachyderma* [*Sagawa et al.*, 2013], as claimed by *Darling et al.* [2006]. Equilibrium offsets for *Globigerinita glutinata* are available from only two studies, but these too show large regional variation, from −0.1‰ to

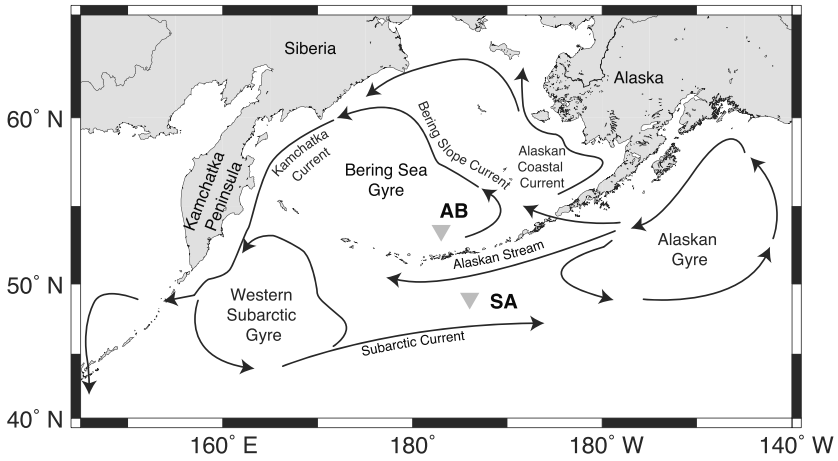

Figure 1. Map showing the locations of sediment trap deployments in the Bering Sea (Station AB) and the central subarctic Pacific (Station SA). Arrows indicate major oceanic surface currents in the study region [*Stabeno et al.*, 1999].

−1.5‰ [*Kahn and Williams*, 1981; *Ločarić et al.*, 2006]. Because there are still only limited regional data available, additional data for the Pacific region can provide further insights into regional differences in $\delta^{18}O_{Foram}$ equilibrium offsets.

In contrast to $\delta^{18}O_{Foram}$, the calibration of $\delta^{13}C_{Foram}$ is still addressing the difficulties of parameterizing responses to environmental conditions. The difficulties are primarily due to the complex mechanisms of calcification in association with species-specific biological activity. Previous studies have implicated several biological factors affecting $\delta^{13}C_{Foram}$ such as (1) metabolic processes (e.g., respiration), (2) photosynthetic activity by symbionts, (3) temperature, and (4) carbonate chemistry [*Spero et al.*, 1997; *Bemis et al.*, 2000; *Bauch et al.*, 2002; *Jonkers et al.*, 2013]. Because such biological effects bias the original $\delta^{13}C$ information in dissolved inorganic carbon ($\delta^{13}C_{DIC}$), fossil $\delta^{13}C_{Foram}$ tends to reflect multiple parameters [*Ravelo and Hillaire-Marcel*, 2007], emphasizing the importance of additional calibration data for $\delta^{13}C_{Foram}$.

Recently, multispecies $\delta^{18}O_{Foram}$ and $\delta^{13}C_{Foram}$ measurements have assisted various environmental reconstructions. A typical application is to evaluate thermal stratification by using the $\delta^{18}O_{Foram}$ signature of multiple species from different habitat depths [*Hillaire-Marcel et al.*, 2001; *Spero et al.*, 2003], under the assumption of relatively stable habitat depths over time. However, *Field* [2004] reported that such an application could easily be biased by seasonal variations in habitat depths. New interpretations of geochemical signatures of multiple planktic foraminifera have been proposed to represent different seasons by using calibration studies based on material collected in sediment traps [*King and Howard*, 2005; *Kuroyanagi et al.*, 2011; *Jonkers et al.*, 2013; *Sagawa et al.*, 2013]. This idea mainly comes from the species-specific seasonality witnessed in flux maxima. The significant seasonal variation in planktic foraminiferal fluxes observed in the Bering Sea and the central subarctic Pacific [*Asahi and Takahashi*, 2007] is background and motivation for this study. Long-term $\delta^{18}O_{Foram}$ and $\delta^{13}C_{Foram}$ records potentially provide further constraints in interpreting multispecies $\delta^{18}O_{Foram}$ and $\delta^{13}C_{Foram}$ data.

There are almost no calibrations for $\delta^{18}O_{Foram}$ and $\delta^{13}C_{Foram}$ from the Bering Sea or the central subarctic Pacific, despite the rising importance of these regions in paleoceanography [e.g., *Takahashi et al.*, 2011] and the application of $\delta^{18}O_{Foram}$ and $\delta^{13}C_{Foram}$ records to paleoceanographic reconstruction [*Schlung et al.*, 2013]. Long-term continuous time series sediment trap deployments and recoveries in the Bering Sea and central subarctic Pacific have produced an archived collection of sinking particle samples for the period 1990–2010 [*Takahashi et al.*, 2012]. The continuous presence of planktic foraminifers in these sediment trap samples [*Asahi and Takahashi*, 2007] permits the establishment of $\delta^{18}O_{Foram}$ and $\delta^{13}C_{Foram}$ records and provides an opportunity to observe their responses to environmental changes.

This paper documents $\delta^{18}O_{Foram}$ and $\delta^{13}C_{Foram}$ of three species for a decade, collected by two time series sediment traps moored in the Bering Sea (from August 1990 to July 1999) and the central subarctic Pacific (from August 1990 to July 2000) (Figure 1). These data are further examined with respect to issues in

paleoceanographic applications by evaluating (1) species-specific $\delta^{18}O_{Foram}$ equilibrium offsets, (2) $\delta^{13}C_{Foram}$ variations with environmental change, (3) seasonal habitat depth, and (4) seasonality recorded in fossil specimens. The new $\delta^{18}O_{Foram}$ and $\delta^{13}C_{Foram}$ data in this study can be used to reconstruct paleoceanographic and paleoenvironmental conditions in the Bering Sea and central subarctic Pacific.

2. Oceanographic Setting and Seasonal Succession of Planktic Foraminifera

The dominant surface water circulation in the Bering Sea is an anticlockwise gyre (the Bering Sea Gyre; Figure 1) [*Stabeno et al.*, 1999]. Most inflows to the Bering Sea from the North Pacific are from the Alaskan Stream, which flows along the southern side of the Aleutian Islands. The eastern side of the Aleutian Basin is strongly influenced by North Pacific water via various northward inflows along the Aleutian Islands [*Kinney and Maslowski*, 2012].

Station SA is located between two major surface currents: the Alaskan Stream to the north and the Subarctic Current to the south (Figure 1). There is a temporal succession in the influence of these two currents [*Ohnishi and Ohtani*, 1999] that has significantly affected the planktic foraminiferal assemblages at Station SA [*Asahi and Takahashi*, 2007]. Furthermore, the two currents are associated with the "Subarctic Front," which separates the northern Pacific subarctic water mass from subtropical water [*Belkin and Mikhaylichenko*, 1986]. The position of the subarctic front varied between 42°N and 47°N from 1977 to 1999 [*Belkin et al.*, 2002]; thus, Station SA was under the influence of the subarctic water mass throughout the study period.

The Bering Sea and central subarctic Pacific are characterized by strong mixing during winter due to winter cooling of surface water. Seasonal temperature changes at the surface ranged from 2.8 to 9.6°C at Station AB and from 4.1 to 11.3°C at Station SA (Figure 2). In comparison, variations in the seasonal salinity (expressed as the mean salinity over the upper 100 m) showed much lower amplitude, from 32.97 to 33.02 at Station AB and from 32.92 to 32.96 at Station SA, in association with the strong permanent halocline in the North Pacific [*Miura et al.*, 2003; *Ueno et al.*, 2005]. These observations suggest that the characteristics of the upper water layers in the study region are likely controlled by temperature changes. Temperature-driven mixing resulted in a seasonal mixed layer depth (MLD) that was deepest during February (96 m at Station AB and 81 m at Station SA) and shallowest in July and August (16 m at Station AB and 15 m at Station SA) (Global Ocean Data Assimilation Database (GODAS) [*Behringer and Xue*, 2004]). Such seasonal mixing drives the supply of nutrients to the euphotic layer, thus regulating seasonal patterns of biological production.

The seasonal patterns of biological production in the Bering Sea and the central subarctic Pacific have been well described in terms of various biological parameters using sediment trap materials collected at Stations AB and SA [*Asahi and Takahashi*, 2007; *Ikenoue et al.*, 2012; *Onodera and Takahashi*, 2009, 2012; *Takahashi et al.*, 2002, 2012]. In response to environmental changes (e.g., nutrient supply via winter mixing and warming of surface water via solar radiation), variations in all parameters examined coincided with two pronounced seasonal flux maxima, during spring and fall at both stations. However, the relative magnitude and duration of each seasonal flux maximum varied with biological taxon. In particular, planktic foraminifera showed species- and region-specific variations along with seasonal flux patterns [*Asahi and Takahashi*, 2007]. *Globigerina umbilicata* showed one pronounced flux maximum during fall at Station AB and two seasonal flux maxima at Station SA, with the primary one during spring and the secondary one during fall. This is in contrast to the flux maxima of *N. pachyderma*, which tended to occur nearly equally during spring and fall throughout the study periods at both stations [*Asahi and Takahashi*, 2007, 2008]. The seasonal flux pattern of *G. glutinata* resembles that of *N. pachyderma*, with two flux maxima appearing equally during spring and fall at both Stations AB and SA. Their relative abundance and flux tend to be higher during relatively warm conditions (high sea surface temperature anomaly) whereas fluxes of other foraminifera are generally low [*Asahi and Takahashi*, 2008]. Such distinct variations in the timing of flux maxima suggest their potential for use in reconstructing different seasonal patterns in the fossil record.

3. Materials and Methods

3.1. Sediment Trap Samples

Sinking particles were collected by two sediment traps (PARFLUX Mark 7G-13 with 13 rotary collectors; *Honjo and Doherty* [1988]) deployed in the Bering Sea (Station AB: 53.5°N, 177°W, trap depth 3200 m) and the

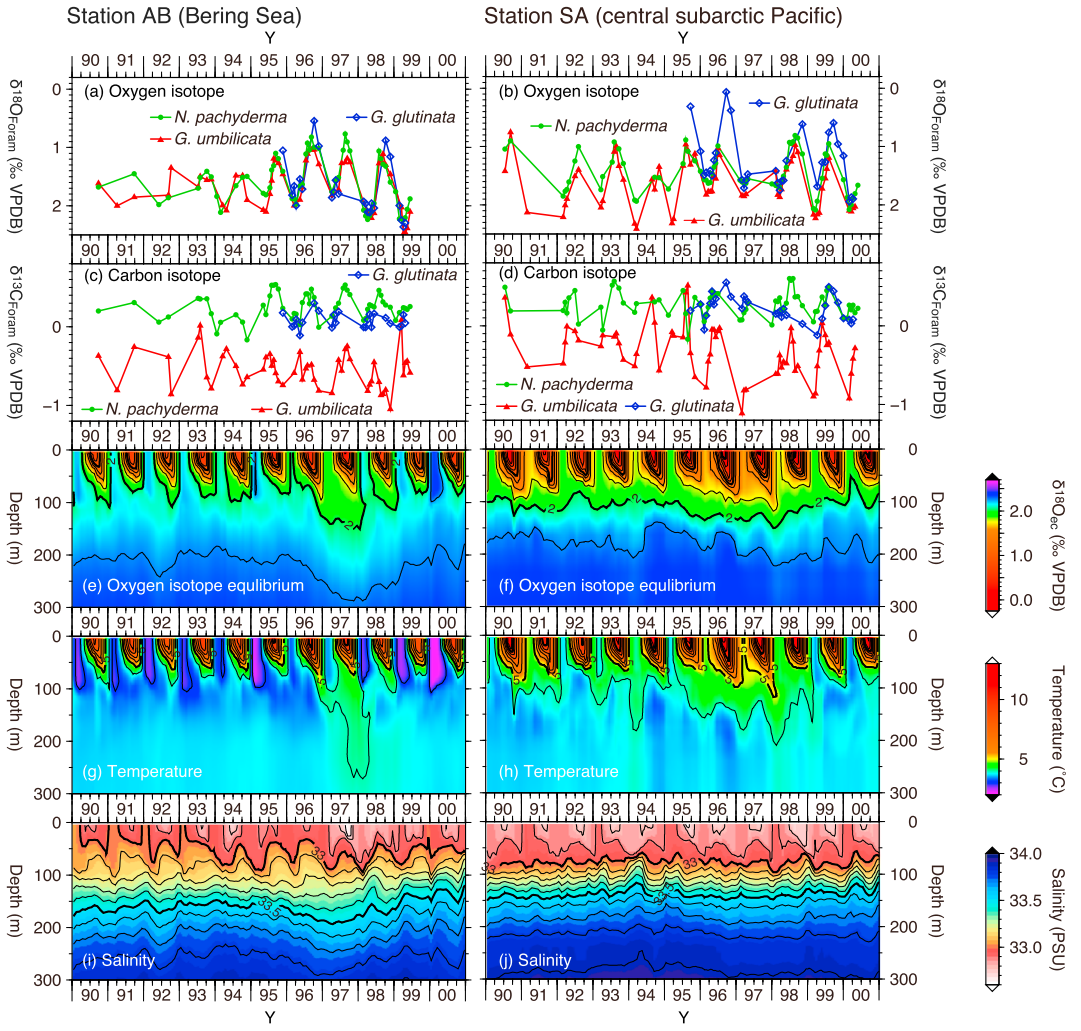

Figure 2. Time series plots of (a, b) $\delta^{18}O_{Foram}$, (c, d) $\delta^{13}C_{Foram}$ at midday of the actual sampling period (i.e., not flux-weighted monthly average), and depth profiles of (e, f) $\delta^{18}O_{ec}$, (g, h) temperature, and (i, j) salinity at Stations AB and SA. Note that $\delta^{18}O_{ec}$ is calculated from the disequilibrium equation of *Kim and O'Neil* [1997] using temperature and salinity data (GODAS: *Behringer and Xue* [2004]) and the regional salinity-$\delta^{18}O_w$ equation for the Pacific [*LeGrande and Schmidt*, 2006]. Thick contour lines represent 1‰ ($\delta^{18}O_{ec}$), 5°C (temperature), and salinity intervals of 0.5, whereas thin lines represent 0.2‰ ($\delta^{18}O_{ec}$), 1°C (temperature), and 0.1 salinity intervals. Each year on the *x* axis is divided into four seasons in sequence, winter, spring, summer, and fall, respectively.

central subarctic Pacific (Station SA: 49°N, 174°W, trap depth 4830 m). A total of nine year-long time series were collected at Station AB and ten at Station SA from August 1990 to July 2010 (Figure 1) [*Takahashi et al.*, 2002]. From this 20 year sampling period, we focused only on samples collected between 1990 and 2000, using exactly the same samples as those described by *Asahi and Takahashi* [2007]. Each sediment trap mooring system was tethered 600 m above the seafloor to avoid collecting resuspended seafloor sediment. The moorings were recovered and redeployed every year from Training Ship (T/S) *Oshoro-Maru* of Hokkaido University. Samples from August 1999 to July 2000 from Station AB are missing because of a failed recovery of the mooring system in 2000.

Sampling intervals varied from 20 to 56 days depending on the seasonal biological production (see *Takahashi et al.* [2012] for further details). Prior to deployment, each sample cup was filled with a preservative consisting of a sodium borate-buffered (pH 7.6–7.8) 5% solution of either glutaraldehyde (1990–1994) or formaldehyde (1995–2000), made with seawater collected from 2000 m depth at the respective stations. The timing of all flux data collected was shifted by 32 days (Station AB) or 48 days (Station SA) under the assumption that the particle sinking speed was around 100 m/d [*Klaas and Archer*, 2002].

3.2. Oxygen and Carbon Isotope Measurements

Among the foraminiferal species found at Stations AB and SA [*Asahi and Takahashi*, 2007], three planktic species were selected for oxygen and carbon isotope measurements: *Neogloboquadrina pachyderma*, *Globigerina umbilicata*, and *Globigerinita glutinata*. *Neogloboquadrina pachyderma* at Stations AB and SA is predominantly the sinistral form (approximately 98%) [*Asahi and Takahashi*, 2007]; thus, all *N. pachyderma* data in this paper are from the sinistral form, representing a single morphologic/genetic variant [*Darling et al.*, 2006]. *Globigerina umbilicata* is a second dominant planktic foraminifer at both stations, and is thought to be a morphologic variation of *Globigerina bulloides*, judging from its thick shell walls and texture [*Ujiié*, 2003; *Asahi and Takahashi*, 2007].

Specimens for isotopic measurement were picked from a 125–250 μm size fraction of a 1/64 aliquot of the original samples. We used samples identical to those used for previously published taxonomic works [*Asahi and Takahashi*, 2007]. At least 15 *N. pachyderma* and *G. glutinata* and 5 *G. umbilicata* specimens were used for isotope measurements. To make our data comparable to other sediment trap studies [*King and Howard*, 2005; *Kuroyanagi et al.*, 2011; *Jonkers et al.*, 2013; *Sagawa et al.*, 2013], we chose a cleaning protocol similar to that applied in those studies. The cleaning procedure involved (1) crushing the shells in a clean glass vial with a clean stainless steel needle, and (2) repeated ultrasonication with Milli-Q water and 99.5% methanol alternately. We made no specific attempts to remove organic matter (e.g., bleaching or plasma ashing) in accordance with recent reports on the minimal effects of organic carbon contamination on isotopes in biogenic carbonate [*Grottoli et al.*, 2005; *Serano et al.*, 2008; *Wierzbowski*, 2007].

Cleaned samples were dried in a clean dry cabinet for 12 h prior to isotope measurements. Oxygen and carbon isotopes were measured on a GV Instruments IsoPrime with the Multicarb preparation system (Wythenshave, Manchester, UK) at the Center for Advanced Marine Core Research, Kochi University. The analytical precision, based on repeated measurements of the NBS-19 standard, was better than ±0.02‰ for $\delta^{13}C_{Foram}$ and ±0.06‰ for $\delta^{18}O_{Foram}$.

3.3. Hydrographic Data

In order to compare isotopic data with associated environmental changes, we collected hydrographic data within a 1° × 1° area around each trap site from globally distributed databases. Monthly temperature and salinity profiles for the upper 500 m of the water column from 1990 to 2000 were taken from the Global Ocean Data Assimilation System database (GODAS; *Behringer and Xue* [2004]), and long-term means of monthly vertical nutrient profiles were taken from the World Ocean Atlas 09 (WOA09; *Garcia et al.* [2010]). There was a strong correlation between actual CTD data collected every August [*Faculty of Fisheries, Hokkaido University*, 1991–2001] and GODAS data, validating the use of GODAS data to represent regional oceanographic conditions (Figure S1 in the supporting information).

The monthly temperature and salinity data, with 10 m vertical resolution, enabled us to estimate temporal changes of oxygen isotopes in the equilibrium state of calcite ($\delta^{18}O_{ec}$) (Figures 2, S3a, and S3e), using the equation of *Kim and O'Neil* [1997]:

$$T\,(^{\circ}C) = 16.10 - 4.64\left(\delta^{18}O_{ec} - \delta^{18}O_w\right) + 0.09\left(\delta^{18}O_{ec} - \delta^{18}O_w\right)^2, \quad (1)$$

where $\delta^{18}O_{ec}$ and $\delta^{18}O_w$ are the $\delta^{18}O$ of calcite and water, respectively. The $\delta^{18}O_w$ was calculated from the relationship between salinity and $\delta^{18}O_w$ in the North Pacific [*LeGrande and Schmidt*, 2006] as follows:

$$\delta^{18}O_w(‰\ \mathrm{VSMOW}) = 0.44 \times \mathrm{salinity} - 15.13. \quad (2)$$

The $\delta^{18}O_w$ on the Vienna Standard Mean Ocean Water (VSMOW) scale was converted into ‰ Vienna Pee Dee Belemnite (VPDB) by subtracting 0.27‰ [*Hut*, 1987].

There is a general difficulty in determining seasonal variations of $\delta^{13}C$, unlike $\delta^{18}O$, because of the limited seasonal data available. Instead, we estimated $\delta^{13}C$ in dissolved inorganic carbon ($\delta^{13}C_{DIC}$) by using an empirical approach. *Jonkers et al.* [2013] used multiple linear regression (MLR) to estimate $\delta^{13}C_{DIC}$ in the North Atlantic. We applied this same approach to the hydrographic datasets provided by the Global Data Analysis Project (GLODAP; *Key et al.* [2004]) and Pacific Ocean Interior Carbon (PACIFICA; *Suzuki et al.* [2013]) for the upper 500 m of the North Pacific (54.2–47.5°N, 163°E–172°W). Those data satisfied the

empirical equations and demonstrated their validity (in terms of correlation coefficient r^2 and root mean square error RMSE) for carbonate chemistry in the upper 500 m of the North Pacific as follows:

$$\begin{aligned}\mathrm{DIC}\left(\ \mu\mathrm{mol\ kg^{-1}}\right) &= -1263.6 + 0.482057\times T + 98.0934\times S + 5.92275\times \mathrm{NO_3} \\ \left(n = 485, r^2 = 0.987,\ \mathrm{RMSE} = 13.32\ \ \mu\mathrm{mol\ kg^{-1}}\right),\end{aligned} \tag{3}$$

$$\begin{aligned}\delta^{13}\mathrm{C_{DIC}}(‰\mathrm{VPDB}) &= -15.383 + 0.019790\times T + 1.1326\times S \\ &\quad - 0.02069\times \mathrm{NO_3} - 0.0097084\times \mathrm{DIC} \\ (n = 28, r^2 = 0.997,\ \mathrm{RMSE} &= 0.0565‰),\end{aligned} \tag{4}$$

and

$$\begin{aligned}\mathrm{ALK}\left(\ \mu\mathrm{mol\ kg^{-1}}\right) &= -682.2 + 1.7419\times T + 88.12\times S - 0.1394\times \mathrm{NO_3} \\ \left(n = 57, r^2 = 0.929,\ \mathrm{RMSE} = 11.22\ \ \mu\mathrm{mol\ kg^{-1}}\right),\end{aligned} \tag{5}$$

where DIC, ALK, T, and S represent dissolved inorganic carbon, alkalinity, temperature, and salinity, respectively. Calculated $\delta^{13}\mathrm{C_{DIC}}$ values were then "time shifted" to an arbitrary time domain, using the value of -0.012 ‰·y^{-1} for the North Pacific [*Tanaka et al.*, 2003] to account for the oceanic uptake of anthropogenic CO_2 from fossil fuel combustion. We also calculated temporal changes in CO_3^{2-} concentrations above 500 m water depth using the predicted and archived dataset and the software "CO2calc" [*Robbins et al.*, 2010].

3.4. Flux-Weighted Averaging of $\delta^{18}\mathrm{O_{Foram}}$ and $\delta^{13}\mathrm{C_{Foram}}$

Flux-weighted averaging is a useful technique for obtaining average isotope values over certain time windows with consideration of seasonal productivity. The most typical application is to evaluate $\delta^{18}\mathrm{O_{Foram}}$ and $\delta^{13}\mathrm{C_{Foram}}$ effects by seasonal variability in planktic foraminifer production [*Kuroyanagi et al.*, 2011; *Sagawa et al.*, 2013]. Because our sampling intervals ranged from 20 to 56 d, we can also use this technique to obtain monthly average $\delta^{18}\mathrm{O_{Foram}}$ and $\delta^{13}\mathrm{C_{Foram}}$ to make our data comparable to oceanographic data sets. Potential bias converting into flux-weighted monthly averages is estimated to be less than or similar to analytical errors (*N. pachyderma*: ±0.05‰ for $\delta^{18}\mathrm{O_{Foram}}$ and ±0.04‰ for $\delta^{13}\mathrm{C_{Foram}}$; *G. umbilicata*: ±0.06‰ for $\delta^{18}\mathrm{O_{Foram}}$ and ±0.07‰ for $\delta^{13}\mathrm{C_{Foram}}$; *G. glutinata*: ±0.06‰ for $\delta^{18}\mathrm{O_{Foram}}$ and ±0.05‰ for $\delta^{13}\mathrm{C_{Foram}}$, respectively).

To calculate the flux-weighted averages, we used measured $\delta^{18}\mathrm{O_{Foram}}$ and $\delta^{13}\mathrm{C_{Foram}}$ together with temporal flux variations at Stations AB and SA [*Asahi and Takahashi*, 2007] and the following equations:

$$\begin{aligned}&\text{Flux-weighted average } \delta^{18}\mathrm{O_{Foram}}(‰\ \mathrm{VPDB}) = \\ &\sum_{i=1}^{n}\left(\mathrm{flux}_i\times\delta^{18}\mathrm{O_{Foram}}_{\ \ i}\right)/\sum_{i=1}^{n}\left(\mathrm{flux}_i\right),\end{aligned} \tag{6}$$

and

$$\begin{aligned}&\text{Flux-weighted average } \delta^{13}\mathrm{C_{Foram}}(‰\ \mathrm{VPDB}) = \\ &\sum_{i=1}^{n}\left(\mathrm{flux}_i\times\delta^{13}\mathrm{C_{Foram}}_{\ \ i}\right)/\sum_{i=1}^{n}\left(\mathrm{flux}_i\right).\end{aligned} \tag{7}$$

We used planktic foraminiferal fluxes within the 125–250 μm size fraction, the same as our $\delta^{18}\mathrm{O_{Foram}}$ and $\delta^{13}\mathrm{C_{Foram}}$ measurements, to minimize any bias due to size fractionation.

4. Results

4.1. Oxygen Isotopic Ratios

Temporal variations in $\delta^{18}\mathrm{O_{Foram}}$ in the three subject species showed similar patterns at the two time series stations (Figures 2 and 3), as confirmed by the strong correlations between $\delta^{18}\mathrm{O_{Foram}}$ of *N. pachyderma* and the other two species at each station (Figures S2a and S2b). The most obvious variations in $\delta^{18}\mathrm{O_{Foram}}$ over the 10 years of sediment trap data were seasonal maxima in February–April and seasonal minima in July–September (Figure 3). The $\delta^{18}\mathrm{O_{Foram}}$ generally followed the estimated $\delta^{18}\mathrm{O_{ec}}$. The seasonal amplitudes of $\delta^{18}\mathrm{O_{Foram}}$ for *N. pachyderma* (0.71‰ at Station AB and 0.87‰ at Station SA) and *G. umbilicata* (0.69‰ at Station AB and 0.93‰ at Station SA) were generally consistent with those for $\delta^{18}\mathrm{O_{ec}}$ between 5 and 95 m water depth (0.78‰ at Station AB and 0.75‰ at Station SA). A similar trend was observed in *G. glutinata*

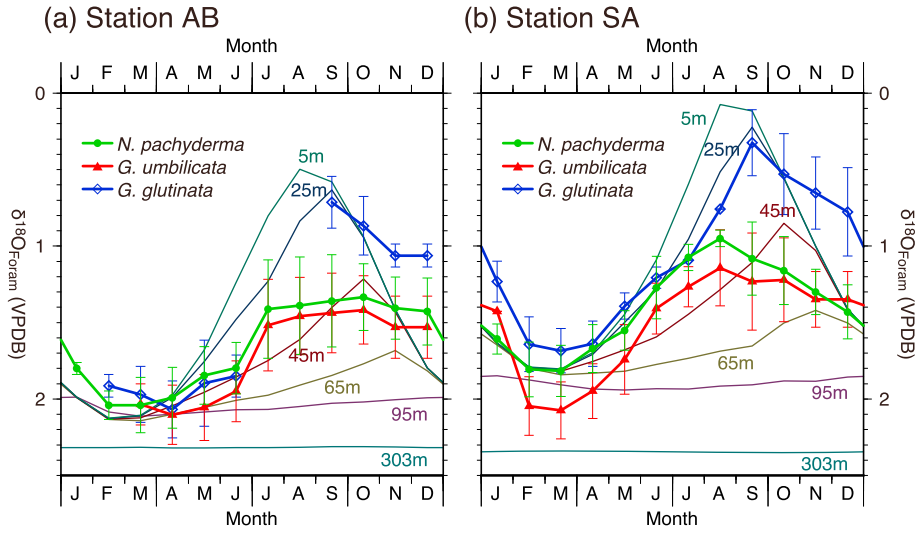

Figure 3. Monthly means from long-term time series of $\delta^{18}O_{Foram}$ (*N. pachyderma*, *G. umbilicata*, and *G. glutinata*) along with $\delta^{18}O_{ec}$ at specific depths (5, 25, 45, 65, 95, 125, 303 m; gray lines) and the MLD, at Stations AB and SA. Error bars indicate standard deviations of $\delta^{18}O_{Foram}$ (*N. pachyderma*, *G. umbilicata*, and *G. glutinata*).

with a shallower water depth range than that of *G. umbilicata*, showing amplitudes (1.35‰ at Station AB and 1.36‰ at Station SA) in close agreement with those of $\delta^{18}O_{ec}$ from 5 to 45 m water depth (1.31‰ at Station AB and 1.37‰ at Station SA). In addition to the seasonal variations, the long-term variations also coincided with those for $\delta^{18}O_{ec}$ (Figure 2). At Station AB the long-term trend for all $\delta^{18}O_{Foram}$ clearly matched the general warming trend in the upper 100 m during 1996–1997 and the subsequent pronounced cooling in winter of 1999 (Figure 2). A similar warming episode during 1995–1998 was also visible at Station SA, as seen in low winter $\delta^{18}O_{Foram}$ for all three species, and low summer $\delta^{18}O_{Foram}$ of *G. glutinata* during 1995–1996. There was no clear evidence of summer warming during 1997–1998 in the $\delta^{18}O_{Foram}$ for any of the three taxa, or during 1996 for *N. pachyderma* or *G. umbilicata*, because low foraminiferal fluxes during these intervals resulted in a lack of data [*Asahi and Takahashi*, 2007].

4.2. Carbon Isotopic Ratios

In contrast to $\delta^{18}O_{Foram}$, $\delta^{13}C_{Foram}$ of *N. pachyderma*, *G. umbilicata*, and *G. glutinata* showed independent, species-specific temporal variations at both stations (Figure 2). The inter-species correlations between $\delta^{13}C_{Foram}$ of *N. pachyderma* and the other two species (*G. umbilicata* and *G. glutinata*) differed from those of $\delta^{18}O_{Foram}$ as follows: $r = 0.22$ (with *G. umbilicata*) and 0.52 (*G. glutinata*) at Station AB, and $r = 0.46$ (*G. umbilicata*) and 0.55 (*G. glutinata*) at Station SA (Figures S2c and S2d). Such a wide variety of correlation coefficients r is a reflection of the species-specific seasonal and long-term trends in observed $\delta^{13}C_{Foram}$. The $\delta^{13}C_{Foram}$ of *G. umbilicata* was markedly lower than those of the other two species at both stations in nearly all years (Figure 2).

The seasonal $\delta^{13}C_{Foram}$ values were highest during summer (July to September) at both stations (Figure 2). The lowest values occurred during winter (January to March) for all datasets except for *G. umbilicata* at Station AB (during November to December), which may be attributable to a lack of winter data. The seasonal amplitudes of $\delta^{13}C_{Foram}$ for *G. umbilicata* were relatively large compared to those of *N. pachyderma* and *G. glutinata*. The $\delta^{13}C_{Foram}$ of *G. umbilicata* also showed a different long-term trend than those of the other taxa (Figure 2), shifting to a mean value of -0.51 ± 0.25‰ during 1997–1999 at Station SA compared to a mean of -0.26 ± 0.29‰ during other periods.

5. Discussion

5.1. Oxygen Isotopes: Equilibrium, Equilibrium Offsets, and Calcification Depths

To parameterize $\delta^{18}O_{Foram}$ responses to their habitats, three major factors need to be constrained: the equations that determine $\delta^{18}O_{Foram}$ at equilibrium with ambient seawater, $\delta^{18}O_{Foram}$ offsets from equilibrium, and habitat or calcification depths. These three factors are addressed in the following sections.

Table 1. Estimated Equilibrium Offsets for *N. pachyderma*, *G. umbilicata* and *G. glutinata* at Stations AB and SA Using Different $\delta^{18}O$ Equilibrium Equations Provided by *Epstein et al.* [1953], *O'Neil et al.* [1969], *Wefer and Berger* [1991], and *Kim and O'Neil* [1997][a]

				Equilibrium Equation							
				Kim and O'Neil [1997]		*Wefer and Berger* [1991]		*O'Neil et al.* [1969]		*Epstein et al.* [1953][b]	
Station	Species	Depth (m)	*n*	Average (‰ VPDB[c])	SD (‰ VPDB)	Average (‰ VPDB)	SD (‰ VPDB)	Average (‰ VPDB)	SD (‰ VPDB)	Average (‰ VPDB)	SD (‰ VPDB)
AB	*N. pachyderma*	5–65	11	0.07	0.11	0.52	0.10	0.52	0.10	0.62	0.09
	G. umbilicata	5–65	6	0.05	0.08	0.50	0.08	0.50	0.08	0.60	0.08
		125	6	0.05	0.11	0.48	0.11	0.48	0.11	0.57	0.11
	G. glutinata	5–65	7	0.14	0.10	0.58	0.09	0.58	0.09	0.69	0.09
SA	*N. pachyderma*	5–65	21	0.00	0.11	0.41	0.11	0.41	0.11	0.48	0.12
	G. umbilicata	5–65	19	−0.25	0.18	0.16	0.18	0.16	0.18	0.23	0.18
		125	19	0.00	0.16	0.42	0.16	0.42	0.16	0.49	0.15
	G. glutinata	5 − 65	12	0.18	0.19	0.59	0.19	0.59	0.19	0.65	0.19
AB and SA combined	*N. pachyderma*	5–65	32	0.02	0.12	0.45	0.12	0.45	0.12	0.53	0.13
	G. umbilicata	5–65	25	−0.18	0.21	0.24	0.22	0.24	0.22	0.32	0.23
		125	25	0.01	0.15	0.43	0.15	0.43	0.15	0.51	0.15
	G. glutinata	5–65	19	0.16	0.16	0.59	0.16	0.59	0.16	0.66	0.16

[a]Note that oxygen isotope equilibrium offsets were estimated from monthly average $\delta^{18}O_{Foram}$ and $\delta^{18}O_{ec}$ during winter (January to March); thus *n* represents the number of winter months used for the estimation.
[b]Includes $\delta^{18}O_w$ offset of 0.2‰ to convert into VPDB scale.
[c]Vienna Pee Dee Belemnite.

5.1.1. Equilibrium Equations and $\delta^{18}O_{Foram}$

While comparing our data to other published data discussing equilibrium status of planktic foraminifers, choice of equation estimating $\delta^{18}O_{ec}$ should be paid great attentions [e.g., *King and Howard,* 2005; *Kuroyanagi et al.*, 2011]. In addition to the equation of *Kim and O'Neil* [1997], there are three equations commonly applied evaluating $\delta^{18}O_{ec}$ [*Epstein et al.,* 1953; *O'Neil et al.*, 1969; *Wefer and Berger*, 1991]. Potential bias by choice of the equation is concerned to be 0.4–0.6‰ at temperature range of our study.

5.1.2. $\delta^{18}O$ Equilibrium Offsets of Planktic Foraminifera

Sediment trap studies have often used winter data to evaluate $\delta^{18}O_{Foram}$ equilibrium offsets [*King and Howard*, 2005; *Kuroyanagi et al.*, 2011; *Jonkers et al.*, 2013; *Sagawa et al.*, 2013]. One major reason for using data from samples collected during winter is that winter mixing eliminates effects of habitat depth differences [*Kuroyanagi et al.*, 2011; *Jonkers et al.*, 2013; *Sagawa et al.*, 2013]. On the basis of the variation of $\delta^{18}O_{ec}$ profiles during winter, we used a $\delta^{18}O_{ec}$ averaged over 5–65 m water depth as a first order approximation for the equilibrium offset (Figures 3, S3a, and S3e).

The estimated equilibrium offsets of *N. pachyderma* were similar at both stations (Station AB, -0.07 ± 0.11‰; Station SA, 0.00 ± 0.11‰). The fairly constant offset above 125 m at both stations indicates that *N. pachyderma* can thrive at any depth within the mixed layer during winter (Table 1 and Figures S3b and S3f). In contrast, the estimated offset approached 0 around 35–55 m water depth during summer, suggesting that the calcification depth of *N. pachyderma* is limited to a certain water depth range during warm stratified periods (Figures S3b and S3f).

Our estimated equilibrium offset of about 0‰ for *N. pachyderma* comprised values from most sediment trap studies, but not those from plankton tow studies, which range up to 1.0‰ (Table 2). This inconsistency in offsets could result from differences in $\delta^{18}O_{ec}$ estimates [*King and Howard*, 2005; *Kuroyanagi et al.*, 2011; *Sagawa et al.*, 2013]. At both stations, estimated offsets differed by as much as 0.4–0.6‰ depending on the $\delta^{18}O_{ec}$ chosen (Table 1).

Another reason for this inconsistency may be $\delta^{18}O_{Foram}$ modification via encrustation [*Kohfeld et al.*, 1996; *Kozdon et al.*, 2009]. Intratest data have shown that the equilibrium offset relative to the $\delta^{18}O_{ec}$ at actual habitat depth is −1.4‰ to −0.6‰ within ontogenetic calcite and +0.8‰ in the encrusted parts [*Kozdon et al.*, 2009]. It is worth noting that inconsistencies in equilibrium offsets have been observed in plankton tow studies and in most sediment trap studies (Table 1). Thus, the $\delta^{18}O_{Foram}$ of sediment trap material could be biased by the inclusion of encrusted parts, compared to less encrusted specimens in plankton tow studies.

Table 2. Planktic Foraminiferal $\delta^{18}O_{ec}$ Equilibrium Offsets From Previous Studies[a]

Reference	Region	Sampling Method	Species	Offset (‰)	Equilibrium Equation
This study	Bering Sea / central subarctic Pacific	Sediment trap	*N. pachyderma (sin.)*	0.0	*Kim and O'Neil* [1997]
		Sediment trap	*G. umbilicata*	0.0	*Kim and O'Neil* [1997]
		Sediment trap	*G. glutinata*	−0.2	*Kim and O'Neil* [1997]
Jonkers et al. [2013]	Northwestern Atlantic	Sediment trap	*N. pachyderma (sin.)*	0.0	*Kim and O'Neil* [1997]
		Sediment trap	*G. bulloides*	0.0	*Kim and O'Neil* [1997]
Kuroyanagi et al. [2011]	Northwestern Pacific	Sediment trap	*N. pachyderma (sin.)*	−1.0	*Wefer and Berger* [1991]
King and Howard [2005]	Southern Ocean	Sediment trap	*N. pachyderma (sin.)*	−0.4	*Epstein et al.* [1953]
			G. bulloides	−0.4	*Epstein et al.* [1953]
			N. pachyderma (sin.)	0.0	*Kim and O'Neil* [1997]
			G. bulloides	0.0	*Kim and O'Neil* [1997]
Sagawa et al. [2013]	Western North Pacific	Sediment trap	*N. pachyderma (sin.)*	0.0	*Kim and O'Neil* [1997]
			G. bulloides	0.0	*Kim and O'Neil* [1997]
Bauch et al. [1997]	Arctic Ocean	Plankton tow, surface sediment	*N. pachyderma (sin.)*	−1.0	*O'Neil et al.* [1969]
Bauch et al. [2002]	Sea of Okhotsk	Plankton tow	*N. pachyderma (sin.)*	−1.0	*O'Neil et al.* [1969]
Kahn and Williams [1981]	Northeastern Pacific	Plankton tow	*G. glutinata*	−1.5[b]	*Kim and O'Neil* [1997]
Kohfeld et al. [1996]	North Atlantic	Plankton tow, sediment trap, surface sediment	*N. pachyderma (sin.)*	−0.8[c]	*O'Neil et al.* [1969]
Kozdon et al. [2009]	North Atlantic	Plankton tow	*N. pachyderma (sin.)*	−1.0	*Epstein et al.* [1953]
Ločarić et al. [2006]	South eastern Atlantic	Plankton tow, sediment trap	*G. glutinata*	−0.1[c]	*Kim and O'Neil* [1997]
Mortyn and Charles [2003]	Southern Ocean	Plankton tow	*N. pachyderma (sin.)*	−1.0	*O'Neil et al.* [1969]
			G. bulloides	−0.9	*O'Neil et al.* [1969]
Simstich et al. [2003]	Nordic Sea	Sedment trap, plankton tow, surface sediment	*N. pachyderma (sin.)*	−0.9[c]	*O'Neil et al.* [1969]
Ortiz et al. [1996]	Northeastern Pacific	Plankton tow	*N. pachyderma (sin.)*	−0.7	*Epstein et al.* [1953]
Volkmann and Mensch [2001]	Laptev Sea (North Atlantic)	Plankton tow	*N. pachyderma (sin.)*	−1.3	*O'Neil et al.* [1969]

[a]The sample collection methods and equilibrium equations are also listed along with the reported equilibrium offsets.
[b]Equilibrium offset was originally evaluated by the equation of *Horibe and Oba* [1972].
[c]Equilibrium offset of plankton tow samples.

This scenario explains most equilibrium offset inconsistencies, except for a sediment trap study in the western North Pacific [*Kuroyanagi et al.*, 2011], suggesting that the degree of encrustation may vary regionally.

In contrast to *N. pachyderma*, the estimated equilibrium offset for *G. umbilicata* using $\delta^{18}O_{ec}$ between 5–65 m water depth was different at Station AB (−0.05 ± 0.08‰) and Station SA (+0.25 ± 0.18‰) (Table 1). The values estimated every 10 m in depth documented this inconsistency down to 100 m at Station SA (Figures S3c and S3g). The potential influence of CO_3^{2-} concentration on $\delta^{18}O_{Foram}$ of *G. bulloides* has been noted in laboratory cultures [*Spero et al.*, 1997]. However, the expected regional contrast in $\delta^{18}O_{Foram}$, resulting from CO_3^{2-} concentrations and the equation of *Spero et al.* [1997], is much lower (0.06 ± 0.12‰) than the difference in equilibrium offsets between Stations AB and SA (0.30 ± 0.26‰). Our findings also compromise a sediment trap study in the Southern Ocean [*King and Howard*, 2005] that argued against the CIE as a minor reason for equilibrium offsets of *G. bulloides*. Instead, we hypothesize that such regional contrasts can be explained by different winter habitat/calcification depths at Stations AB and SA. The equilibrium offset at Station SA is compatible with that at Station AB if we assume a calcification/habitat depth in winter extending down to around 125 m (Table 1 and Figures S3c and S3g). If we allow for a small CIE relative to the observed regional contrast in equilibrium offsets for *G. umbilicata*, their winter habitat/calcification depth at Station SA could be much deeper than in waters affected by surface mixing.

The wide range of equilibrium offsets reported for *G. bulloides* (Table 2) can also be explained by modification of its $\delta^{18}O_{Foram}$ via encrustation. The major criteria differentiating *G. umbilicata* from *G. bulloides* are based on its shell structure and thick, occasionally encrusted shell [*Ujiié*, 2003; *Asahi and Takahashi*, 2007]. Thus the $\delta^{18}O_{Foram}$ of *G. umbilicata* at Stations AB and SA could be modified via encrustation. Furthermore, *G. umbilicata* characterizes the subarctic waters of the North Pacific, and some specimens reported as *G. bulloides* might arguably be reclassified as *G. umbilicata* [*Ujiié*, 2003]. The finding of similar equilibrium offsets for *G. bulloides* (or *G. umbilicata*) from sediment trap studies in the subarctic and subantarctic realms [*King and Howard*, 2005; *Jonkers et al.*, 2013; *Sagawa et al.*, 2013; this study] may reflect measurements from similarly encrusted specimens. Future taxonomic work is required to test this hypothesis.

As with *N. pachyderma*, equilibrium offsets for *G. glutinata* were similar at both stations (Table 1 and Figure S3), suggesting that this species survives throughout the mixed layer during winter. A similar equilibrium offset was reported from a plankton tow study in the southeastern Atlantic [*Ločarić et al.*, 2006], with lower $\delta^{18}O_{Foram}$ for *G. glutinata* compared to $\delta^{18}O_{ec}$, suggesting no modification of $\delta^{18}O_{Foram}$ via encrustation. However, an equilibrium offset for the northeastern Pacific [*Kahn and Williams*, 1981] had a substantially different value (−1.6‰), leaving room for further evaluation of additional regional and methodological variations.

5.1.3. Habitat Depths of Planktic Foraminifera in the Bering Sea and the Central Subarctic Pacific: A Simple Comparison by $\delta^{18}O_{Foram}$

As seen in the estimated equilibrium offsets for *G. umbilicata*, it is possible that each species differs in its seasonal habitat or calcification depth (hereafter, calcification depth). The temporal variability in calcification depths was estimated for each foraminifer by comparing the $\delta^{18}O_{ec}$ to the measured $\delta^{18}O_{Foram}$ (Figures 2, 4, and S3).

The seasonal variation in calcification depth of *N. pachyderma* showed its clear preference for calcifying between 35 and 55 m during summer at both stations (Figures 4, S3b, and S3f). Deepening of the calcification depth was seen clearly at Station SA and less clearly at Station AB (Figure 4). The large uncertainty in the winter calcification depth at Station AB is primarily because of the homogeneity of $\delta^{18}O_{ec}$ (2.15 ± 0.11‰) down to around 300 m water depth resulting from winter mixing (Figures 2, S3a, and S3e). In comparison, winter mixing at Station SA is shallower, down to around 80 m (Figures S3a and S3e). A statistically confirmed smaller $\delta^{18}O_{ec}$ above 80 m (1.75 ± 0.15‰) than below 80 m (2.16 ± 0.17‰) indicates the separation of those two water zones, leading to smaller variation in their estimated winter calcification depth (Figures 4 and S3). We found some samples with $\delta^{18}O_{Foram}$ outside the range of $\delta^{18}O_{ec}$ above 300 m (Figures 2 and 4). These samples were considered to be remnants from the warm season, analogous to those found in other sediment trap studies [*Jonkers et al.*, 2010, 2013; *Sagawa et al.*, 2013]. Excluding these outliers, the temporal variation in calcification depth of *N. pachyderma* was well correlated with the MLD ($r = 0.72$, $p < 0.001$, $n = 61$ at Station AB; $r = 0.76$, $p < 0.001$, $n = 62$ at Station SA) (Figure S4).

The seasonal calcification depth of *G. umbilicata* showed more variation than that of *N. pachyderma* (Figure 4). The estimated winter equilibrium offsets at Station SA approached 0‰ only at 125 m water depth (Figure S3c and S3g). On the other hand, during summer an equilibrium offset around 0‰ was seen at depths of 35–55 m (Figures S3c and S3g), implying that the calcification depth of *G. umbilicata* may vary seasonally. Possibly because of the homogeneity of the upper water column, the shoaling of the calcification depth of *G. umbilicata* was delayed until June–July at Station AB, whereas it occurred during May–June at Station SA. As with *N. pachyderma*, samples of *G. umbilicata* with lower $\delta^{18}O_{Foram}$ than surface $\delta^{18}O_{ec}$ were considered remnants from the warm season. However, some samples had apparent calcification depths greater than 300 m (Figure 4). Because $\delta^{18}O_{ec}$ below 300 m was very homogeneous at Stations AB (2.37 ± 0.05‰) and SA (2.39 ± 0.05‰), even the analytical error for $\delta^{18}O_{Foram}$ measurements (0.06‰) generates a large uncertainty in their estimated calcification depth. Again, by excluding these outliers the temporal variation in *G. umbilicata* calcification depth was reasonably well correlated with the MLD ($r = 0.41$, $p < 0.001$, $n = 61$ at Station AB; $r = 0.81$, $p < 0.001$, $n = 61$ at Station SA) (Figure S4).

The calcification depth of *G. glutinata* was clearly different at Stations AB and SA. Excluding the outliers, as with *N. pachyderma* and *G. umbilicata*, the relationship between calcification depth and MLD was only visible at Station SA ($r = 0.81$, $p < 0.001$, $n = 23$) (Figure S4). The low correlation at Station AB ($r = 0.42$, $p = 0.07$, $n = 20$) was mainly due to a deep estimated calcification depth during winter (Figure 4), implying a possible unknown mechanism increasing $\delta^{18}O_{Foram}$ of *G. glutinata* relative to $\delta^{18}O_{ec}$ at Station AB. Alternatively, this wide range of estimated calcification depths may simply result from the limited data availability. Additional data for *G. glutinata* are desirable.

In contrast to winter, the calcification depth of *G. glutinata* during summer stayed at 25–35 m at both stations (Figure 4). A greater frequency of samples with $\delta^{18}O_{Foram}$ lower than surface $\delta^{18}O_{ec}$ indicates that the *G. glutinata* calcification depth was shallower than those of *N. pachyderma* and *G. umbilicata*.

Despite the wide range of actual reported calcification depths from different regions, there is general agreement that the calcification depths of *N. pachyderma* and *G. bulloides* are close to the regional MLD in cold-water regions (e.g., *Volkmann and Mensch* [2001] in the Fram Strait; *Bauch et al.* [2002] in the Sea of Okhotsk). In addition, seasonal variations in the habitat depths of these taxa were evident in a

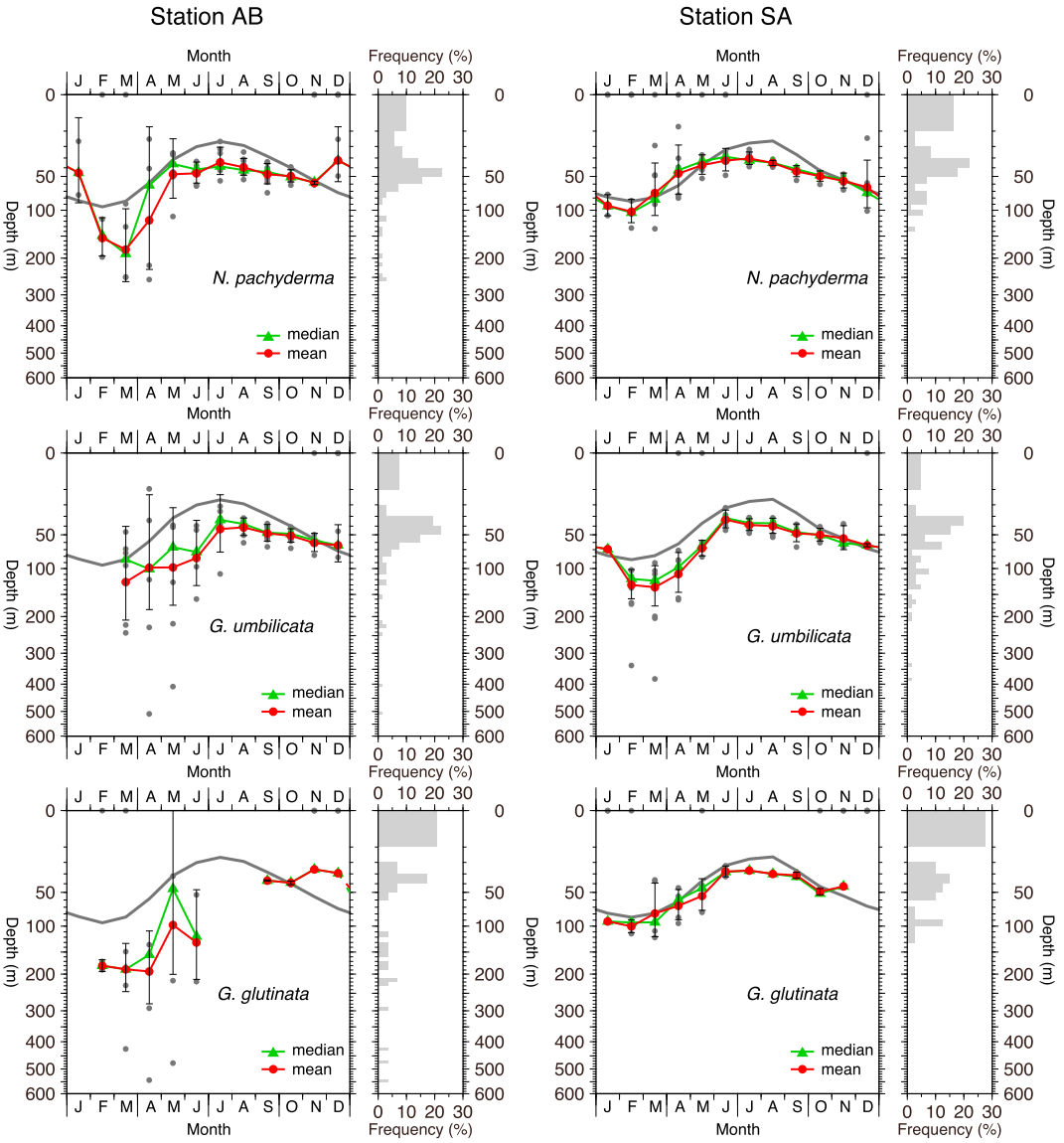

Figure 4. Monthly means and frequency distributions of habitat/calcification depths of three planktic foraminifera at Stations AB and SA. Lines represent means (red) and medians (green) of actual depth estimates (shown as gray dots), and depth of the mixed layer (thick gray lines). Gray histograms represent relative abundance with depth. Data from estimated depths deeper than 300 m or shallower than 5 m are excluded from long-term means and medians. The habitat depths were estimated from the $\delta^{18}O_{ec}$ (Figure 2), the species-specific equilibrium offset (Table 1), and the measured $\delta^{18}O_{Foram}$ of each taxa. Data showing the $\delta^{18}O_{Foram}$ lower than $\delta^{18}O_{ec}$ at the surface are plotted at 0 m. Error bars indicate standard deviations of estimated habitat/calcification depth.

multiple-season plankton tow study off the coast of southern California, USA [*Field*, 2004], lending support to our estimated calcification depths that change along with the MLD. In sediment trap studies, such a seasonal deepening of calcification depths during winter is observed as a difference of about 20 m [*Kuroyanagi et al.*, 2011; *Sagawa et al.*, 2013]. The smaller seasonal variations in calcification depths found in previous studies, compared to our estimates, are likely associated with the homogeneity of $\delta^{18}O_{ec}$ during the cold season. Relatively deep winter mixing occurs at high latitudes in the North Pacific [*Suga et al.*, 2004]. We suspect that winter mixing in our study region is stronger than elsewhere, thus small changes in $\delta^{18}O_{Foram}$ can equate to large differences in estimated calcification depths. Even with such an uncertainty in the estimates, evidence from sediment trap studies across the North Pacific provides a clear indication of the seasonal calcification depth variability around the MLD.

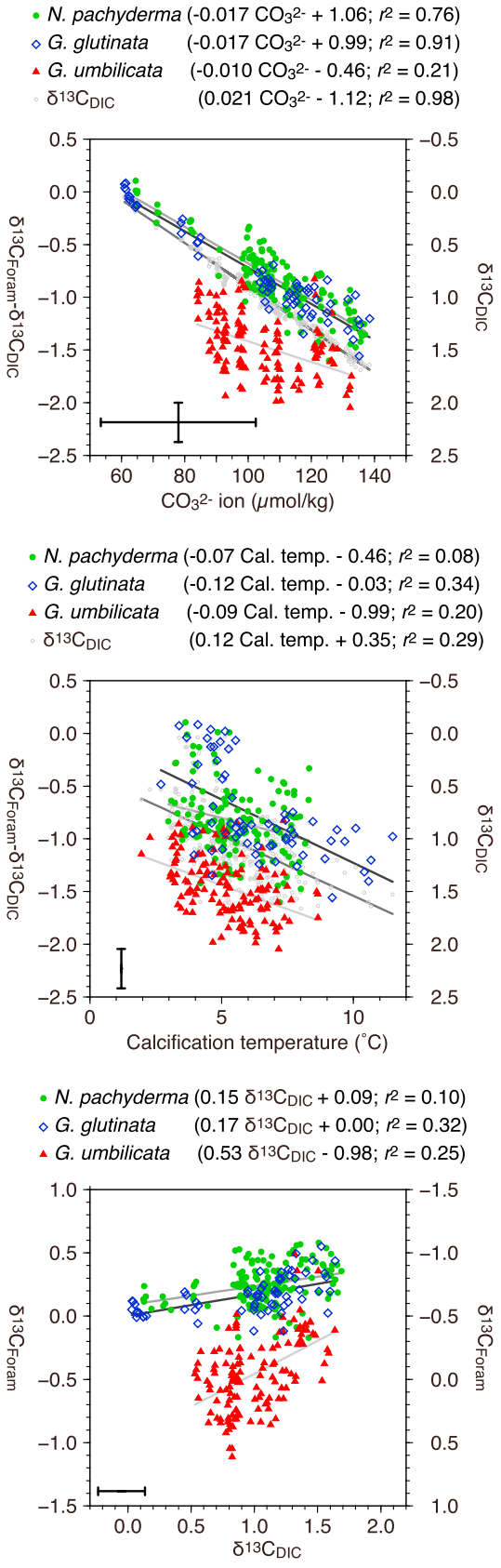

5.2. Carbon Isotope Response to Environmental Changes

Ambient temperature and CO_3^{2-} concentrations are two major factors regulating $\delta^{13}C_{Foram}$ [e.g., *Spero et al.*, 1997; *Bemis et al.*, 2000; *Bauch et al.*, 2002; *King and Howard*, 2004]. Our $\delta^{13}C_{Foram}$ data show greater potential correspondence to carbonate chemistry than to temperature change (Figures 5a–5c). Moreover, *G. umbilicata* shows a greater response to carbonate chemistry in the water column than the other two species (Figures 5c and 6).

The large seasonal variation in $\delta^{13}C_{DIC}$ (around 1.5‰) makes it difficult to precisely evaluate $\delta^{13}C_{Foram}$ responses to environmental changes, because any signal in foraminifer shells would likely be masked this variation. Moreover, $\delta^{13}C_{DIC}$ is regulated by a variety of environmental factors, so any estimated $\delta^{13}C_{Foram}$ response to environmental change would likely be inaccurate because of the large seasonal $\delta^{13}C_{DIC}$ variations. *Jonkers et al.* [2013] pointed out the difficulty in distinguishing the influence of temperature on $\delta^{13}C_{Foram}$ because of the strong correlation between temperature and $\delta^{13}C_{DIC}$ ($r = 0.94$).

A typical example of such an overestimate is evident in the plot of the difference between $\delta^{13}C_{Foram}$ and $\delta^{13}C_{DIC}$ ($\delta^{13}C_{Foram\text{-}DIC}$) versus CO_3^{2-} concentrations (Figure 5a). This plot shows the significant correlations for *N. pachyderma* ($r = -0.87$, $n = 144$) and *G. glutinata* ($r = -0.95$, $n = 65$), likely resulting from the strong correlation between CO_3^{2-} concentrations and $\delta^{13}C_{DIC}$ ($r = 0.99$, $n = 693$). Furthermore, the slopes of the regression lines for this relationship for *N. pachyderma* and *G. glutinata* (both -0.017 ± 0.001 ‰·[μmol kg^{-1}]$^{-1}$) are almost identical (but opposite in sign) to the slope for the relationship between $\delta^{13}C_{DIC}$ and CO_3^{2-} (0.020 ± 0.001 ‰·[μmol kg^{-1}]$^{-1}$), indicating that their high correlations are simply derived from the $\delta^{13}C_{DIC}$–CO_3^{2-} relationship, not by any changes

Figure 5. Comparison plots of the $\delta^{13}C_{Foram\text{-}DIC}$ disequilibrium versus (a) CO_3^{2-} versus (b) calcification temperature and (c) the $\delta^{13}C_{Foram}$–$\delta^{13}C_{DIC}$ relationship of *N. pachyderma*, *G. umbilicata*, and *G. glutinata* at Stations AB and SA. The calcification temperatures were calculated from measured $\delta^{18}O_{Foram}$ and $\delta^{18}O_w$, using the equilibrium equation of *Kim and O'Neil* [1997]. Note that $\delta^{13}C_{DIC}$ values were calculated for the long-term mean seasonal calcification depths (Figure 4). Error bar at each panel is estimated from RMSE of MLR estimation of the carbonate chemistry in ambient water (see section 3.3 for further details).

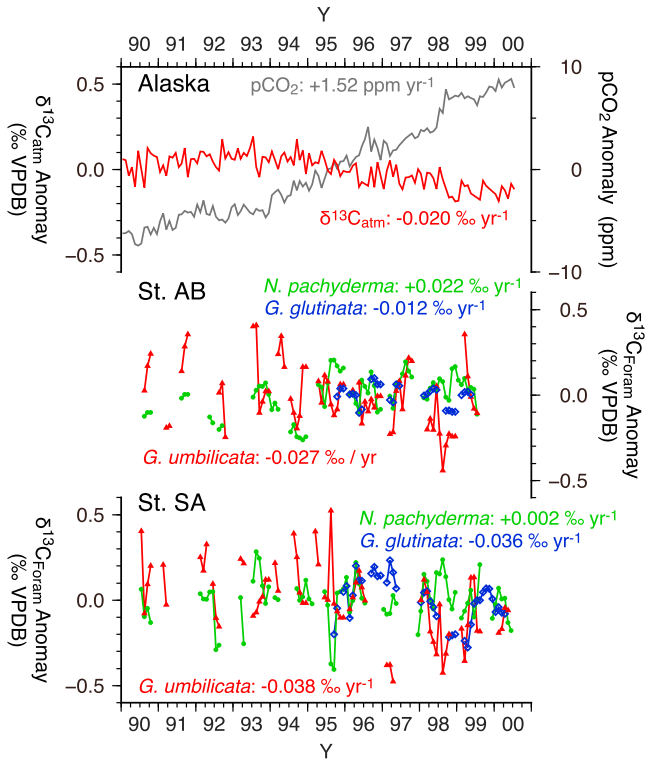

Figure 6. Time series anomaly plots of pCO_2 and $\delta^{13}C_{atm}$ at Point Barrow, Alaska, USA. [*Keeling et al.*, 2005], and monthly average $\delta^{13}C_{Foram}$ of *N. pachyderma*, *G. umbilicaa*, and *G. glutinata* at Stations AB and SA. All anomalies are calculated based on their 1990–1999 means.

in $\delta^{13}C_{Foram}$ in response to changes in CO_3^{2-} concentration (Figure 5a).

Despite the difficulties of evaluating $\delta^{13}C_{Foram}$ responses to any environmental factors, Figures 5a and 5b still provide insightful information. The disequilibrium with CO_3^{2-} concentration is evidence that *G. umbilicata* $\delta^{13}C_{Foram}$ responds to carbonate chemistry. The slope of the relationship between the difference between $\delta^{13}C_{Foram}$ and $\delta^{13}C_{DIC}$ ($\delta^{13}C_{Foram\text{-}DIC}$) and CO_3^{2-} concentrations for *G. umbilicata* (-0.010 ± 0.002 ‰·[μmol kg^{-1}]$^{-1}$) is significantly different from those for *N. pachyderma* and *G. glutinata*, reflecting an apparent response to changes in CO_3^{2-} concentrations (Figure 5a). This slope differs from the slope of the $\delta^{13}C_{DIC}$–CO_3^{2-} relationship by -0.011 ‰·[μmol kg^{-1}]$^{-1}$), almost the same as the CIE in *G. bulloides* (-0.012 to -0.014 ‰·[μmol kg^{-1}]$^{-1}$) [*Spero et al.*, 1997; *Peeters et al.*, 2002].

The relatively weak correlations between $\delta^{13}C_{Foram\text{-}DIC}$ and temperature for all species in this study suggest that temperature is less important to $\delta^{13}C_{Foram}$ changes than CO_3^{2-} concentration (Figure 5b). The strongest correlation between $\delta^{13}C_{Foram\text{-}DIC}$ and temperature is for *G. glutinata* ($r = -0.58$, slope $= -0.12 \pm 0.02$‰·°C^{-1}, $p < 0.001$), likely owing to the large variation in this species' seasonal calcification depth (Figure 4). In comparison, the correlations between $\delta^{13}C_{Foram\text{-}DIC}$ of *N. pachyderma* or *G. umbilicata* and temperature are even weaker (*N. pachyderma*, $r = -0.28$, slope $= -0.07 \pm 0.02$ ‰·°C^{-1}, $p < 0.001$; *G. umbilicata*, $r = -0.45$, slope $= -0.09 \pm 0.02$ ‰·°C^{-1}, $p < 0.001$).

A second piece of evidence for species-specific $\delta^{13}C_{Foram}$ responses to carbonate chemistry is the relationship between $\delta^{13}C_{Foram}$ and $\delta^{13}C_{DIC}$ (Figure 5c). The regression of these parameters for *G. umbilicata* yields a slope of 0.53 ± 0.08, greater than those for *N. pachyderma* (0.15 ± 0.04) and *G. glutinata* (0.17 ± 0.03), suggesting a measurable response of *G. umbilicata* $\delta^{13}C_{Foram}$ to carbonate chemistry. Such species-specific responses to $\delta^{13}C_{DIC}$ could be associated with different habitats and diets, or with activity and metabolism of symbionts. Only *G. glutinata* in this study is known to harbor facultative symbionts [*Kucera*, 2007]. Because photosynthetic activity sequesters low $\delta^{13}C_{DIC}$ from respired CO_2 in internal carbon pools [*Ravelo and Hillaire-Marcel*, 2007], the $\delta^{13}C_{Foram}$ of symbiont-bearing foraminifers should be higher than that of non-symbiont-bearing taxa [*Bemis et al.*, 2000]. The relatively low slope for the $\delta^{13}C_{Foram}$–$\delta^{13}C_{DIC}$ relationship of *G. glutinata* is likely attributable to this phenomenon.

This photosynthetic activity, however, cannot explain the low slope of the $\delta^{13}C_{DIC}$–$\delta^{13}C_{Foram}$ relationship in the symbiont-free *N. pachyderma* [*Kucera*, 2007]. Culture experiments with specimens collected off Mutsu, Japan, showed that *N. pachyderma* (dextral) can survive solely on algal prey by attaching them to its shell surface, whereas *G. bulloides* survives by feeding on *Artemia salina* (nauplii) [*Kimoto et al.*, 2003]. Algae attached to the *N. pachyderma* shell could bias or dilute the $\delta^{13}C_{DIC}$ in ambient seawater through photosynthesis in the same way that algal symbionts affect the internal carbon pool. These findings suggest a complex mechanism behind the $\delta^{13}C_{Foram}$ of *N. pachyderma* and *G. glutinata*, whereas $\delta^{13}C_{Foram}$ of *G. umbilicata* can be explained by much simpler mechanisms.

The strong response of *G. umbilicata* $\delta^{13}C_{Foram}$ to changes in carbonate chemistry is also supported by the long-term decreasing trend of $\delta^{13}C_{Foram}$ in conjunction with atmospheric $\delta^{13}C$ ($\delta^{13}C_{atm}$) change (Figure 6). Oceanic $\delta^{13}C_{DIC}$ is expected to trend along with the decrease in $\delta^{13}C_{atm}$ due to the addition of anthropogenic CO_2. The Suess effect, expressed as an annual rate of apparent oceanic $\delta^{13}C_{DIC}$ change, is approximately -0.012 ‰ $\cdot y^{-1}$ in the western North Pacific [*Tanaka et al.*, 2003]. Although there is large regional variation in the reported Suess effect, there is general consensus that most oceanic $\delta^{13}C_{DIC}$ is decreasing over time [e.g., *Gruber et al.*, 2002; *Tanaka et al.*, 2003; *Keeling et al.*, 2004; *Quay et al.*, 2007; *Watanabe et al.*, 2011]. Because foraminifera incorporate DIC from ambient water, a similar trend is expected in $\delta^{13}C_{Foram}$. Two of the studied species had negative slopes for $\delta^{13}C_{Foram}$ over time, the steepest for *G. umbilicata* (Station AB, -0.027 ± 0.008 ‰ $\cdot y^{-1}$; Station SA, -0.038 ± 0.008 ‰ $\cdot y^{-1}$) followed by *G. glutinata* (Station AB, -0.012 ± 0.009 ‰ $\cdot y^{-1}$; Station SA, -0.036 ± 0.013 ‰ $\cdot y^{-1}$). The fact that the slope for *G. umbilicata* is steeper than that of $\delta^{13}C_{atm}$ (-0.020 ‰ $\cdot y^{-1}$) and the reported Suess effect (-0.012 ‰ $\cdot y^{-1}$; *Tanaka et al.* [2003]) strongly suggests a response of *G. umbilicata* $\delta^{13}C_{Foram}$ to carbonate chemistry of ambient seawater (Figure 6). In contrast, changes over time in $\delta^{13}C_{Foram}$ of *N. pachyderma* show negligibly small slopes (Station AB, $+0.022 \pm 0.005$ ‰ $\cdot y^{-1}$; Station SA, $+0.002 \pm 0.006$ ‰ $\cdot y^{-1}$), implying that other factors override the original $\delta^{13}C_{DIC}$ signal; thus, *N. pachyderma* $\delta^{13}C_{Foram}$ may not be an appropriate proxy for reconstructing carbonate chemistry. On the other hand, *G. umbilicata* $\delta^{13}C_{Foram}$ showed a clear response to changing $\delta^{13}C_{atm}$, as observed in the moderate correlation between the nonseasonal anomaly of *G. umbilicata* $\delta^{13}C_{Foram}$ and that of $\delta^{13}C_{atm}$ (Station AB, $r = 0.27$, $n = 63$, $p = 0.029$; Station SA, $r = 0.42$, $n = 62$, $p < 0.001$) (Figure 6). Together with other reported evidence [*Hirons et al.*, 2001; *Williams et al.*, 2011], the steeper slope of *G. umbilicata* $\delta^{13}C_{Foram}$ over time reflects the distinct long-term shift in carbonate chemistry in the Bering Sea and the central subarctic Pacific.

The regional contrast between $\delta^{13}C_{Foram}$ of *G. umbilicata* and the other two species at Stations AB and SA (Figure 7) highlights its greater utility as a carbonate chemistry proxy. The seasonal flux pattern of *G. umbilicata* yields an estimated flux-weighted $\delta^{13}C_{Foram}$ of -0.54 ± 0.22‰ at Station AB and -0.31 ± 0.32‰ at Station SA. This regional contrast (higher by 0.23‰ at Station SA) coincides with the difference in flux-weighted estimates of $\delta^{13}C$ in the ambient seawater (higher by 0.18‰ at Station SA). The other two species showed smaller differences in the flux-weighted $\delta^{13}C_{Foram}$ between the two stations (Figure 7) with values much lower than the expected difference as estimated from $\delta^{13}C_{DIC}$ and CO_3^{2-} at the MLD (*N. pachyderma*, 0.49‰; *G. glutinata*, 0.70‰; both higher at Station SA). This contradiction between measured and expected $\delta^{13}C_{Foram}$ of *N. pachyderma* and *G. glutinata* results partly from $\delta^{13}C_{DIC}$ changes in their internal carbon pools from photosynthetic activity by algal symbionts or prey, as discussed earlier in this section. In contrast, the regional contrast between $\delta^{13}C_{Foram}$ of *G. umbilicata*, consistent with regional differences in $\delta^{13}C_{DIC}$ and CO_3^{2-}, strongly supports its applicability as a proxy for carbonate water chemistry in the Bering Sea and the central subarctic Pacific.

5.3. Validity of Multiple-Species $\delta^{18}O_{Foram}$ for Reconstructing Specific Seasons

The consideration of seasonal variations in planktic foraminiferal flux along with $\delta^{18}O_{Foram}$ values can further constrain paleoceanographic information preserved in sediments. Based on variations in species-specific seasonal flux, recent sediment trap studies have argued for the suitability of multiple-species $\delta^{18}O_{Foram}$ and $\delta^{13}C_{Foram}$ measurements to extract information about environmental conditions for specific seasons [*King and Howard*, 2005; *Kuroyanagi et al.*, 2011; *Sagawa et al.*, 2013; *Jonkers et al.*, 2013]. Our results are consistent with these previous studies, but the uncertainty in seasonal flux patterns requires considerable attention.

At Stations AB and SA, the flux maxima of planktic foraminifera occurred during spring and fall, with a variation in prominence of a spring or fall peak depending on the species and station [*Asahi and Takahashi*, 2007]. Variation in seasonal flux patterns provides the opportunity to test a new approach for differentiating seasonal signals by using measurements from multiple species. In the case of *N. pachyderma*, the estimated flux-weighted average $\delta^{18}O_{Foram}$ was 1.62 ± 0.37‰ at Station AB and 1.42 ± 0.35‰ at Station SA (Figure 7). The similarity between these flux-weighted averages and its simple mean (1.59 ± 0.37‰ at Station AB and 1.42 ± 0.34‰ at Station SA) suggests that the $\delta^{18}O_{Foram}$ of *N. pachyderma* in sediments mostly represents the annual mean value. This can be mainly attributed to this taxon's nearly equivalent flux maxima during March–June and September–October.

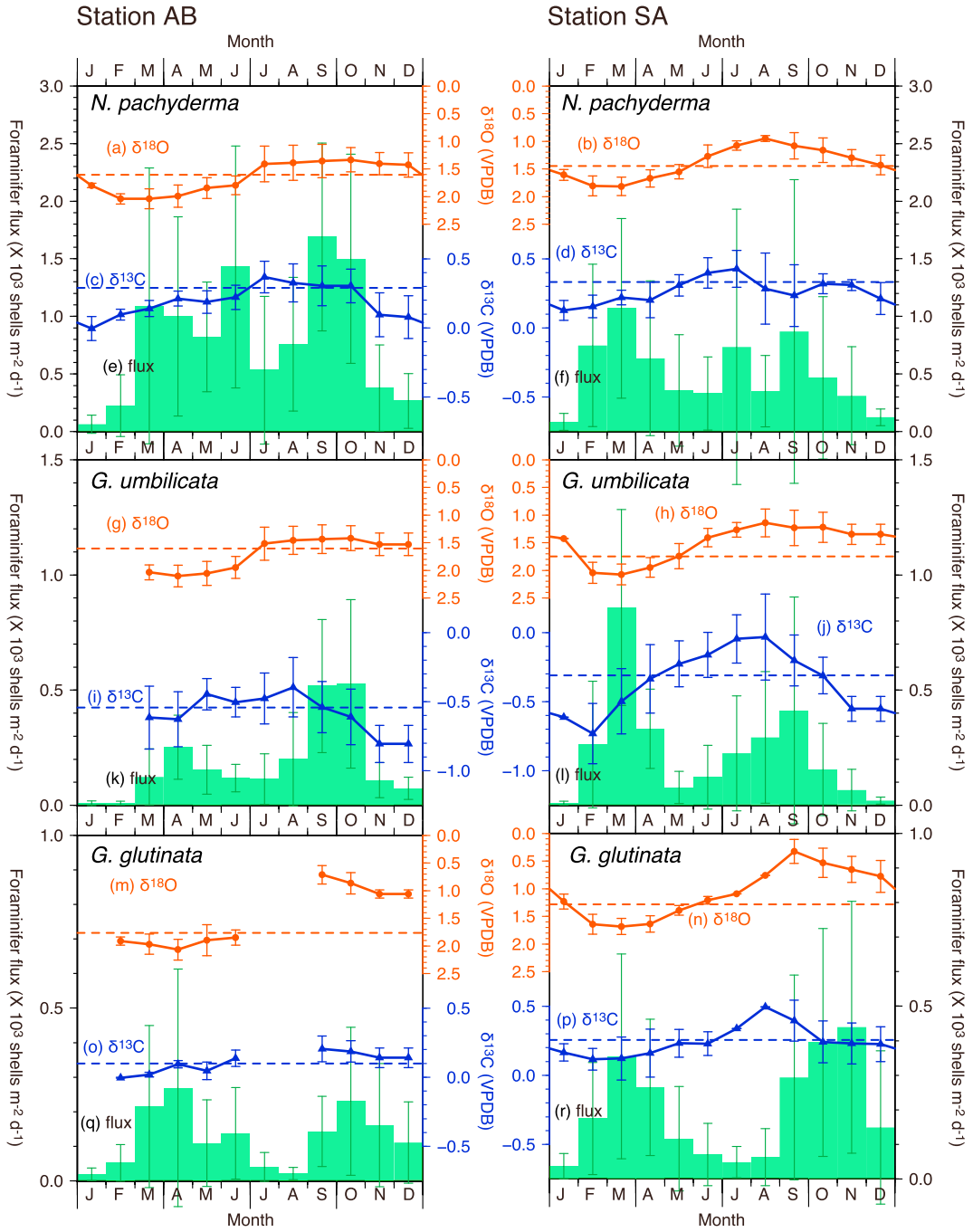

Figure 7. Monthly means of $\delta^{18}O_{Foram}$, $\delta^{13}C_{Foram}$, and flux of *N. pachyderma*, *G. umbilicata*, and *G. glutinata* at Stations (left) AB and (right) SA. Dashed lines represent flux-weighted means of $\delta^{18}O_{Foram}$ and $\delta^{13}C_{Foram}$ at each station. Error bars indicate standard deviations of $\delta^{18}O_{Foram}$, $\delta^{13}C_{Foram}$, and flux, respectively.

Our conclusion that core-top *N. pachyderma* $\delta^{18}O_{Foram}$ represents the annual mean $\delta^{18}O_{Foram}$ at Stations AB and SA generally agrees with observations in the North Atlantic and North Pacific [*Kuroyanagi et al.*, 2011; *Jonkers et al.*, 2013]; however, this is not consistent with other sediment trap studies. For example, *Sagawa et al.* [2013] determined that core-top $\delta^{18}O_{Foram}$ of *N. pachyderma* in the western North Pacific more likely reflected summer subsurface water, whereas *King and Howard* [2005] found the timing of *N. pachyderma* flux maxima varied regionally from austral spring (October to September at 44°S) to summer (January at 47°S and 51°S) in the Southern Ocean. Such regional inconsistencies imply that taking *N. pachyderma* $\delta^{18}O_{Foram}$ as

representative of the annual mean $\delta^{18}O_{Foram}$ is applicable only in the subarctic Pacific and North Atlantic under the assumption that their past and present seasonal flux patterns are similar.

Similar characteristics can be seen in *G. glutinata* at Station AB, with comparable flux-weighted average $\delta^{18}O_{Foram}$ (1.60 ± 0.55‰) and simple mean (1.57 ± 0.53‰), showing that $\delta^{18}O_{Foram}$ in sediments tends to represent the annual mean $\delta^{18}O_{Foram}$ (Figure 7). At Station SA, however, the flux-weighted average of *G. glutinata* $\delta^{18}O$ (1.60 ± 0.45‰) was slightly lower than the simple mean (1.65 ± 0.39‰), a difference nearly within the range of analytical error (0.06‰). This is likely an artifact resulting from the limited data available during summer at Station SA (Figure 7). Therefore, as with *N. pachyderma*, the $\delta^{18}O_{Foram}$ of *G. glutinata* in sediments likely represents the annual mean $\delta^{18}O_{Foram}$.

The flux-weighted average $\delta^{18}O_{Foram}$ of *G. umbilicata* shows potential for representing specific seasons at both stations (Figure 7). At both Stations AB and SA there were differences between the flux-weighted average and simple mean $\delta^{18}O_{Foram}$, suggesting strong seasonality in the $\delta^{18}O_{Foram}$. At Station AB, the slightly lower flux-weighted average (1.59 ± 0.35‰) relative to the simple mean (1.67 ± 0.36‰) indicates that core-top $\delta^{18}O_{Foram}$ for this species represents the annual mean to warm season values. It is relevant that this taxon's primary seasonal flux maximum, in late summer to fall (August to October), accounts for about 56% of its annual flux. In contrast, at Station SA the seasonal flux maxima of *G. umbilicata* appeared primarily during February to April followed by a secondary maximum during June to September (Figure 2), composing 51% (spring) and 33% (summer) of annual flux [*Asahi and Takahashi*, 2007]. The primary flux maximum during spring results in the flux-weighted average $\delta^{18}O_{Foram}$ (1.69 ± 0.43‰) slightly higher than the simple mean (1.60 ± 0.43‰), indicating that core-top records would reflect environmental conditions for cold seasons (late winter to early spring). Note that the flux-weighted average $\delta^{18}O_{Foram}$ of *G. umbilicata* at Station SA was substantially higher than at Station AB, even though conditions at Station SA were about 2°C warmer (Figure 1). Such findings imply that $\delta^{18}O_{Foram}$ for *G. umbilicata* could be used to extract data for specific seasons (annual mean to fall values in the Bering Sea and late winter to early spring in the central subarctic Pacific).

The timing of the *G. umbilicata* seasonal flux maxima was fall at Station AB and spring at Station SA. This variation may be due to the balance between preferred temperature and food availability for *G. umbilicata* in the subarctic Pacific [*Asahi and Takahashi*, 2007]. The major maxima in total mass flux at Stations AB and SA are mainly during spring [*Takahashi et al.*, 2002, 2012]. *Asahi and Takahashi* [2007] argued that cold-water conditions in the Bering Sea during spring delay the growth of *G. umbilicata* at Station AB despite the food availability. On the other hand, the slightly warmer temperatures at Station SA (about 1°C warmer than at Station AB) are within the preferred temperature range of *G. umbilicata*, and the timing of the flux maximum at Station SA is more likely affected by food availability. Such a shift in the timing of primary flux maximum from fall to spring can cause an increase in core-top *G. umbilicata* $\delta^{18}O_{Foram}$ up to around 0.3‰ (Figure 7). The variation in seasonal flux patterns of *G. umbilicata* at Station SA is larger than that at Station AB, suggesting that the *G. umbilicata* fossil record in the central subarctic Pacific could be biased by the shift in the timing of flux maxima due to food availability. In contrast, the fairly consistent fall flux maxima at Station AB shows that fossil *G. umbilicata* $\delta^{18}O_{Foram}$ may be more useful for representing fall signals in the relatively cold Bering Sea. Our findings of uncertainties in seasonal production show that the use of multispecies $\delta^{18}O_{Foram}$ requires careful attention to such uncertainty in the flux timing for reconstructing specific seasons.

6. Conclusions

The 10 year time series sediment trap record of planktic foraminiferal $\delta^{18}O_{Foram}$ and $\delta^{13}C_{Foram}$ reflects environmental changes in the Bering Sea (Station AB) and the central subarctic Pacific (Station SA). Comparisons of $\delta^{18}O_{Foram}$ and $\delta^{13}C_{Foram}$ data with respect to environmental conditions indicate the usability of stable isotopic data for paleoceanographic reconstruction in the subarctic Pacific as follows.

1. $\delta^{18}O_{Foram}$ follows the equilibrium equation of *Kim and O'Neil* [1997] with species-specific equilibrium offsets (*N. pachyderma*, −0.02 ± 0.12‰; *G. umbilicata*, −0.01 ± 0.15‰; *G. glutinata*, −0.16 ± 0.16‰).
2. Contradictions in the $\delta^{18}O_{Foram}$ equilibrium offsets of *N. pachyderma* and *G. bulloides* (*G. umbilicata*) between plankton tow studies (around −0.5 to 1.0‰) and sediment trap studies (around 0.0‰) mostly result from encrustation at greater depths. The seasonal variability in $\delta^{18}O_{Foram}$ evident in all published sediment trap studies indicates that the encrustation process only affects the offset, but likely does not obscure the original $\delta^{18}O_{Foram}$ information in ontogenetic calcite.

3. The calcification or habitat depth can vary seasonally from 35–55 m (*N. pachyderma* and *G. umbilicata*) or 15–35 m (*G. glutinata*) during the warm/stratified season (July to December) to 0–100 m during the cold/well-mixed season (January to June). A deepening of the calcification depth simultaneous with deepening of the MLD to around 100 m points toward the preference of these taxa to be slightly deeper than the MLD.
4. Among the three planktic foraminiferal taxa studied, $\delta^{13}C_{Foram}$ of *G. umbilicata* reflects information most relevant to the carbonate chemistry of ambient seawater. The strong response of *G. umbilicata* $\delta^{13}C_{Foram}$ to carbonate chemistry is evident in (a) the disequilibrium between $\delta^{13}C_{Foram\text{-}DIC}$ and CO_3^{2-}, (b) the $\delta^{13}C_{Foram}$–$\delta^{13}C_{DIC}$ dependence, and (c) $\delta^{13}C_{Foram}$ following the long-term decreasing trend of $\delta^{13}C_{atm}$. These observations strongly support the usability of *G. umbilicata* $\delta^{13}C_{Foram}$ as a proxy for past CO_3^{2-} concentrations. In contrast, the $\delta^{13}C_{Foram}$ of *N. pachyderma* and *G. glutinata* are likely biased by either their algal prey (*N. pachyderma*) or by symbionts (*G. glutinata*), in which photosynthetic activity may alter $\delta^{13}C_{DIC}$ in the internal carbon pool.
5. The flux-weighted average of $\delta^{18}O_{Foram}$ shows the potential use of multispecies fossil $\delta^{18}O_{Foram}$ to reconstruct specific seasons. Core-top $\delta^{18}O_{Foram}$ of *N. pachyderma* and *G. glutinata* likely represent annual mean $\delta^{18}O_{Foram}$, whereas that of *G. umbilicata* mainly reflects annual mean to fall conditions in the Bering Sea (Station AB) and spring in the central subarctic Pacific (Station SA). Unlike $\delta^{18}O_{Foram}$, regional differences in flux-weighted average $\delta^{13}C_{Foram}$ were only evident in *G. umbilicata* and *G. glutinata*, not in *N. pachyderma*. Distinct regional differences in flux-weighted average $\delta^{13}C_{Foram}$ of *G. umbilicata* corresponded to those of $\delta^{13}C_{DIC}$ and CO_3^{2-} at the MLD, strongly suggesting its usability as a proxy for carbonate chemistry of ambient seawater.

Acknowledgments

All data presented in this study can be obtained by contacting either the first author (HA: asahiro@kopri.re.kr) or the corresponding author (BKK: bkkhim@pusan.ac.kr). We are grateful to the captains, officers, crew, scientists and students who participated in a total of 11 cruises during 1989–2000 for sediment trap deployment and recovery on board T/S *Oshoro-Maru* IV of Hokkaido University. In particular, we thank Yoshiaki Maita, Mitsuru Yanada, and Hiroji Ohnishi, of the Graduate School of Fisheries of Hokkaido University, for their dedication in pursuing this bilateral United States-Japan international sediment trap project. Dorinda Ostermann, formerly of Woods Hole Oceanographic Institution, assisted in sediment trap deployments and recoveries on board during the initial stage of the time series experiment. HA and YO thank Michiyo Kobayashi, a former technical support member at the Center for Advanced Marine Core Research (CMCR), for isotope measurements. We also appreciate the critical and constructive comments and suggestion of two reviewers for the improvement of data interpretation. This study was performed under the cooperative research program of CMCR (19-A-23 and 20-A-30). This research was supported by the Japan Society for the Promotion of Science (JSPS) KAKENHI (grant numbers 07680562, 10480128, 17310009 and 30244875 to KT, and 24310019 to YO) of the Ministry of Education, Science and Culture of Japan; the Basic Research Program by the Korea Polar Research Institute (KOPRI) (Grant PE15062 to SIN) and the Excellent Foreigner Post-Doc Invitation Program (Grant PE15220 to SIN), for a postdoctoral position for HA at KOPRI; by the Atmospheric See-At Technology Development Program (grant KMIPA 2015–6060 to BKK).

References

Asahi, H., and K. Takahashi (2007), A 9-year time-series of planktonic foraminifer fluxes and environmental change in the Bering sea and the central subarctic Pacific Ocean, 1990–1999, *Prog. Oceanogr.*, *72*, 343–363.

Asahi, H., and K. Takahashi (2008), A new insight into oceanography with multivariate and time-series analyses on the 1990–1999 planktonic foraminiferal fluxes in the Bering Sea and the central subarctic Pacific, *Mem. Fac. Sci., Kyushu Univ., Ser. D: Geol.*, *32*(1), 73–96.

Bauch, D., J. Carstens, and G. Wefer (1997), Oxygen isotope composition of living *Neogloboquadrina pachyderma* (sin.) in the Arctic Ocean, *Earth Planet. Sci. Lett.*, *146*, 47–58.

Bauch, D., H. Erlenkeuser, G. Winckler, G. Pavlova, and J. Thiede (2002), Carbon isotopes and habitat of polar planktic foraminifera in the Okhotsk Sea: The 'carbonate ion effect' under natural conditions, *Mar. Micropaleontol.*, *45*, 83–99.

Behringer, D., and Y. Xue (2004), Evaluation of the global ocean data assimilation system at NCEP: The Pacific Ocean, paper presented at 8th Symposium on Integrated Observing and Assimilation Systems for Atmosphere, Oceans, and Land Surface, Am. Meteorol. Soc., Seattle, Wash., 11–15 Jan.

Belkin, I., and Y. G. Mikhaylichenko (1986), Thermohaline structure of the Northwest Pacific Frontal Zone near 160°E, *Oceanology*, *26*(1), 47–49.

Belkin, I., R. Krishfield, and S. Honjo (2002), Decadal variability of the North Pacific Polar Front: Subsurface warming versus surface cooling, *Geophys. Res. Lett.*, *29*(9), 1351, doi:10.1029/2001GL013806.

Bemis, B. E., H. J. Spero, J. Bijima, and D. W. Lea (1998), Reevaluation of the oxygen isotopic composition of planktonic foraminifera: Experimental results and revised paleotemperature equations, *Paleoceanography*, *13*, 150–160, doi:10.1029/98PA00070.

Bemis, B. E., H. J. Spero, D. W. Lea, and J. Bijima (2000), Temperature influence on the carbon isotopic composition of *Globigerina bulloides* and *Orbulina universa* (planktonic foraminifera), *Mar. Micropaleontol.*, *38*, 213–228.

Darling, K. F., M. Kucera, D. Kroon, and C. M. Wade (2006), A resolution for the coiling direction paradox in *Neogloboquadrina pachyderma*, *Paleoceanography*, *21*, PA2011, doi:10.1029/2005PA001189.

Epstein, S., R. Buchsbaum, H. A. Lowenstam, and H. C. Urey (1953), Revised carbonate-water isotopic temperature scale, *Bull. Geol. Soc. Am.*, *64*, 1315–1326.

Faculty of Fisheries, Hokkaido University (1991–2001), *Data Record of Exploratory Fishing*, Nos. 34–43, Hokkaido Univ., Hakodate, Japan.

Field, D. B. (2004), Variability in vertical distribution of planktonic foraminifera in the California Current: Relationships to vertical ocean structure, *Paleoceanography*, *19*, PA2014, doi:10.1029/2003PA000970.

Garcia, H. E., R. A. Locarnini, T. P. Boyer, J. I. Antonov, M. M. Zweng, O. K. Baranova, and D. R. Johnson (2010), in *World Ocean Atlas 2009, Volume 4: Nutrients (phosphate, nitrate, silicate)*, *NOAA Atlas NESDIS*, vol. 71, edited by S. Levitus, 398 pp., U.S. Government Printing Office, Washington, D. C.

Grottoli, A. G., L. J. Rodrigues, K. A. Matthews, J. E. Parady, and O. T. Gribb (2005), Pre-treatment effect on coral skeletal $\delta^{13}C$ and $\delta^{18}O$, *Chem. Geol.*, *221*, 225–242.

Gruber, N., C. D. Keeling, and N. R. Bates (2002), Interannual variability in the North Atlantic Ocean Carbon Sink, *Science*, *298*, 2374–2378.

Hillaire-Marcel, C., A. de Vernal, G. Bilodeau, and A. J. Weaver (2001), Absence of deep-water formation in the Labrador Sea during the last interglacial period, *Nature*, *410*, 1073–1077.

Hirons, A. C., D. M. Schell, and B. P. Finney (2001), Temporal records of $\delta^{13}C$ and $\delta^{15}N$ in North Pacific pinnipeds: Inferences regarding environmental change and diet, *Oecologia*, *129*, 591–601.

Honjo, S., and K. W. Doherty (1988), Large aperture time-series sediment traps: Design objectives, construction and application, *Deep Sea Res.*, *35*, 53–97.

Horibe, Y., and T. Oba (1972), Temperature scales of aragonite - water and calcite - water systems, *Paleontol. Soc. Jpn.*, *23–24*, 69–79.

Hut, G. (1987), *Consultants' Group Meeting on Stable Isotope Reference Samples for Geochemical and Hydrological Investigations*, 42 pp., Int. Atomic Energy Agency, Vienna.

Ikenoue, T., K. Takahashi, and S. Tanaka (2012), Fifteen year time-series of radiolarian fluxes and environmental conditions in the Bering Sea and the central subarctic Pacific, 1990–2005, *Deep Sea Res., Part II*, *61–64*, 17–49.

Jonkers, L., G. A. Brummer, F. J. C. Peeters, H. M. van Aken, and M. F. De Jong (2010), Seasonal stratification, shell flux, and oxygen isotope dynamics of left-coiling *N. pachyderma* and *T. quinqueloba* in the western subpolar North Atlantic, *Paleoceanography*, *25*, PA2204, doi:10.1029/2009PA001849.

Jonkers, L., S. van Heuven, R. Zahn, and J. C. Peeters (2013), Seasonal pattern do shell flux, $\delta^{18}O$ and $\delta^{13}C$ of small and large *N. pachyderma* (s) and *G. bulloides* in the subpolar North Atlantic, *Paleoceanography*, *28*, 1–11, doi:10.1002/palo.20018.

Kahn, M., and D. F. Williams (1981), Oxygen and carbon isotopic composition of living planktonic foraminifera from the Northeast Pacific Ocean, *Palaeogeogr. Palaeoclimatol. Palaeoecol.*, *33*, 47–69.

Keeling, C. D., H. Brix, and N. Gruber (2004), Seasonal and long-term dynamics of the upper ocean carbon cycle at station ALOHA near Hawaii, *Global Biogeochem. Cycles*, *18*, GB4006, doi:10.1029/2004GB002227.

Keeling, C. D., S. C. Piper, R. B. Bacastow, M. Wahlen, T. P. Whorf, M. Heimann, and H. A. Meijer (2005), Atmospheric CO_2 and $^{13}CO_2$ exchange with the terrestrial biosphere and oceans from 1978 to 2000: Observations and carbon cycle implications, in *A History of Atmospheric CO_2 and its effects on Plants, Animals, and Ecosystems*, edited by J. R. Ehleringer, T. E. Cerling, and M. D. Dearing, pp. 83–113, Springer, New York.

Key, R. M., A. Kozyr, C. L. Sabine, K. Lee, R. Wanninkhof, J. L. Bullister, R. A. Feely, F. J. Millero, C. Mordy, and T. H. Peng (2004), A global ocean carbon climatology: Results from Global Data Analysis Project (GLODAP), *Global Biogeochem. Cycles*, *18*, GB4031, doi:10.1029/2004GB002247.

Kim, S.-T., and J. R. O'Neil (1997), Equilibrium and nonequilibrium oxygen isotope effects in synthetic carbonates, *Geochim. Cosmochim. Acta*, *61*, 3461–3475.

Kimoto, K., X. Xu, N. Ahagon, H. Nishizawa, and Y. Nakamura (2003), Culturing protocol and maintenance for living calcareous plankton ~ Preliminary results of the culturing experiment ~, *Jpn. Mar. Sci. Technol. Cent.*, *48*, 155–164.

King, A. L., and W. R. Howard (2004), Planktonic foraminiferal $\delta^{13}C$ records from Southern Ocean sediment traps: New estimates of the oceanic Suess effect, *Global Biogeochem. Cycles*, *18*, GB2007, doi:10.1029/2003GB002162.

King, A. L., and W. R. Howard (2005), $\delta^{18}O$ seasonality of planktonic foraminifera from Southern Ocean sediment traps: Latitudinal gradients and implications for paleoclimate reconstructions, *Mar. Micropaleontol.*, *56*, 1–24.

Kinney, J. C., and W. Maslowski (2012), On the oceanic communication between the Western Subarctic Gyre and the deep Bering Sea, *Deep Sea Res., Part I*, *66*, 11–25.

Klaas, C., and D. E. Archer (2002), Association of sinking organic matter with various types of mineral ballast in the deep sea: Implications for the rain ratio, *Global Biogeochem. Cycles*, *16*(4), 1116, doi:10.1029/2001GB001765.

Kohfeld, K. E., R. G. Fairbanks, S. L. Smith, and I. D. Walsh (1996), *Neogloboquadrina pachyderma* (sinistral coiling) as paleoceanographic tracers in polar oceans: Evidence from Northeast Polynya plankton tows, sediment traps, and surface-sediments, *Paleoceanography*, *11*(6), 679–699, doi:10.1029/96PA02617.

Kozdon, R., T. Ushikubo, N. T. Kita, M. Spicuzza, and J. W. Valley (2009), Intratest oxygen isotope variability in the planktonic foraminifer *N. pachyderma*: Real vs. apparent vital effects by ion microprobe, *Chem. Geol.*, *258*, 327–337.

Kucera, M. (2007), Chapter Six Planktonic Foraminifera as Tracers of Past Oceanic Environments, in *Developments in Marine Geology*, vol. 1, edited by C. Hillaire–Marcel and A. De Vernal, pp. 213–262, Elsevier, Amsterdam, doi:10.1016/S1572-5480(07)01011-1.

Kuroyanagi, A., H. Kawahata, and H. Nishi (2011), Seasonal variation in the oxygen isotopic composition of different-sized planktonic foraminifer *Neogloboquadrina pachyderma* (sinistral) in the northwestern North Pacific and implications for reconstruction of the paleoenvironment, *Paleoceanography*, *26*, PA4215, doi:10.1029/2011PA002153.

LeGrande, A. N., and G. A. Schmidt (2006), Global gridded data set of the oxygen isotopic composition in seawater, *Geophys. Res. Lett.*, *33*, L12604, doi:10.1029/2006GL026011.

Ločarić, N., F. J. C. Peeters, D. Kroon, and G.-J. Brummer (2006), Oxygen isotope ecology of recent planktic foraminifera at the central Walvis Ridge (SE Atlantic), *Paleoceanography*, *21*, PA3009, doi:10.1029/2005PA001207.

McConnaughey, T. A., J. Burdett, J. F. Whelan, and C. K. Paull (1997), Carbon isotopes in biological carbonates: Respiration and photosynthesis, *Geochim. Cosmochim. Acta*, *61*(3), 611–622.

Miura, T., T. Suga, and K. Hanawa (2003), Numerical study of formation of dichothermal water in the Bering Sea, *J. Oceanogr.*, *59*, 369–376.

Mortyn, P. G., and C. D. Charles (2003), Planktonic foraminiferal depth habitat and $\delta^{18}O$ calibrations: Plankton tow results from the Atlantic sector of the Southern Ocean, *Paleoceanography*, *18*(2), 1037, doi:10.1029/2001PA000637.

Ohnishi, H., and K. Ohtani (1999), On seasonal and Year to Year variation in flow of the Alaskan Stream in the Central North Pacific, *J. Oceanogr.*, *55*, 597–608.

O'Neil, J. R., R. N. Clayton, and T. K. Mayeda (1969), Oxygen isotope fractionation in divalent metal carbonates, *J. Chem. Phys.*, *51*, 5547–5558.

Onodera, J., and K. Takahashi (2009), Long-term diatom fluxes in response to oceanographic conditions at Stations AB and SA in the central subarctic Pacific and the Bering Sea, 1990–1998, *Deep Sea Res., Part I*, *56*(2), 189–211.

Onodera, J., and K. Takahashi (2012), Oceanographic conditions influencing silicoflagellate flux assemblages in the Bering Sea and subarctic Pacific Ocean during 1990–1994, *Deep Sea Res., Part II*, *61–64*, 4–16.

Ortiz, J. D., A. C. Mix, W. Rugh, J. M. Watkins, and R. W. Collier (1996), Deep-dwelling planktonic foraminifera of the northeastern Pacific Ocean reveal environmental control of oxygen and carbon isotopic disequilibria, *Geochim. Cosmochim. Acta*, *60*, 4509–4523.

Peeters, F. J. C., G.-J. A. Brummer, and G. Ganssen (2002), The effect of upwelling on the distribution and stable isotope composition of *Globigerina Bulloides* and *Globigerinoides Ruber* (planktic foraminifera) in modern surface waters of the NW Arabian Sea, *Global Planet. Change*, *34*(3–4), 269–291.

Quay, P., R. Sonnerup, J. Stutsman, J. Maurer, A. Körtzinger, X. A. Padin, and C. Robinson (2007), Anthropogenic CO_2 accumulation rates in the North Atlantic Ocean from changes in the $^{13}C/^{12}C$ of dissolved inorganic carbon, *Global Biogeochem. Cycles*, *21*, GB1009, doi:10.1029/2006GB002761.

Ravelo, A. C., and C. Hillaire-Marcel (2007), Chapter Eighteen the use of oxygen and carbon isotopes of foraminifera in Paleoceanography, in *Developments in Marine Geology*, vol. 1, edited by C. Hillaire–Marcel and A. De Vernal, pp. 735–764, Elsevier, Amsterdam, doi:10.1016/S1572-5480(07)01023-8.

Robbins, L. L., M. E. Hansen, J. A. Kleypas, and S. C. Meylan (2010), CO2calc—A user-friendly seawater carbon calculator for Windows, Max OS X, and iOS (iPhone), *U.S. Geol. Surv. Open-File Rep.*, 2010–1280, 17 p.

Romanek, C. S., E. L. Grossman, and J. W. Morse (1992), Carbon isotopic fractionation in synthesis aragonite and calcite: Effects of temperature and precipitation rate, *Geochim. Cosmochim. Acta*, *56*, 419–430.

Sagawa, T., A. Kuroyanagi, T. Irino, M. Kuwae, and H. Kawahata (2013), Seasonal variations in planktonic foraminiferal flux and oxygen isotopic composition in the western North Pacific: Implications for paleoceanographic reconstruction, *Mar. Micropaleontol.*, *100*, 11–20.

Schlung, S. A., et al. (2013), Millennial-scale climate change and intermediate water circulation in the Bering Sea from 90 ka; A high-resolution record from IODP Site U1340, *Paleoceanography*, *28*, 54–67, doi:10.1029/2012PA002365.

Serano, O., L. Serano, and M. A. Mateo (2008), Effects of sample pre-treatment of the $\delta^{13}C$ and $\delta^{18}O$ values of living benthic foraminifera, *Chem. Geol.*, *257*, 218–220.

Simstich, J., M. Sarnthein, and H. Erlenkeuser (2003), Paired $\delta^{18}O$ signals of *Neogloboquadrina pachyderma* (s) and *Turborotalita quinqueloba* show thermal stratification structure in Nordic Seas, *Mar. Micropaleontol.*, *48*, 107–125.

Spero, H. J., J. Bijma, D. W. Lea, and B. E. Bemis (1997), Effect of sea-water carbonate concentration on foraminiferal carbon and oxygen isotopes, *Nature*, *390*, 497–500.

Spero, H. J., K. M. Mielke, E. M. Kalve, D. W. Lea, and D. K. Pak (2003), Multispecies approach to reconstructing eastern equatorial Pacific thermocline hydrography during the past 360 kyr, *Paleoceanography*, *18*(1), 1022, doi:10.1029/2002PA000814.

Stabeno, P. J., J. D. Schumacher, and K. Ohtani (1999), The physical oceanography of the Bering Sea, in *Dynamics of the Bering Sea: A Summary of Physical, Chemical, and Biological Characteristics, and a Synopsis of the Bering Sea*, edited by T. R. Loughlin and K. Ohtani, pp. 1–28, North Pacific marine Science Organization (PICES), Univ. of Alaska Sea Grant, Fairbanks, Alaska.

Suga, T., K. Motoki, Y. Aoki, and A. M. Macdonald (2004), The North Pacific climatology of winter mixed layer and mode waters, *J. Phys. Oceanogr.*, *34*, 3–22.

Suzuki, T., et al. (2013), PACIFICA Data Synthesis Project, *ORNL/CDIAC-159, NDP-092*. Carbon Dioxide Information Analysis Center, Oak Ridge National Laboratory, U.S. Department of Energy, Oak Ridge, Tenn., doi:10.3334/CDIAC/OTG.PACIFICA_NDP092.

Takahashi, K., N. Fujitani, and M. Yanada (2002), Long term monitoring of particle fluxes in the Bering Sea and the central subarctic Pacific Ocean, 1990–2000, *Prog. Oceanogr.*, *55*(1–2), 95–112.

Takahashi, K., A. C. Ravelo, C. A. Alvarez-Zarikian, and the Expedition 323 Scientists (2011), *Bering Sea Paleoceanography*, *Proc. IODP Exped. Rep.*, vol. 323, Integr. Ocean Drill. Program Manage. Int., Inc., Tokyo, doi:10.2204/iodp.proc.323.2011.

Takahashi, K., H. Asahi, Y. Okazaki, J. Onodera, H. Tsutsui, T. Ikenoue, Y. Kanematsu, T. Seiji, and S. Iwasaki (2012), Museum archives of the 19 years long time-series sediment trap samples collected at central subarctic Pacific Station SA and Bering Sea Station AB during 1990–2010, *Mem. Fac. Sci., Kyushu Univ., Ser. D: Geol.*, *32*(4), 1–39.

Tanaka, T., Y. W. Watanabe, S. Watanabe, and S. Noriki (2003), Oceanic Suess effect of $\delta^{13}C$ in subpolar region: The North Pacific, *Geophys. Res. Lett.*, *30*(22), 2159, doi:10.1029/2003GL018503.

Ueno, H., E. Oka, T. Suga, and H. Onishi (2005), Seasonal and interannual variability of temperature inversions in the subarctic North Pacific, *Geophys. Res. Lett.*, *32*, L20603, doi:10.1029/2005GL23948.

Ujiié, H. (2003), A 370-ka paleoceanographic record from the Hess Rise, central North Pacific Ocean, and an indistinct 'Kuroshio Extension', *Mar. Micropaleontol.*, *49*(1–2), 21–47.

Volkmann, R., and M. Mensch (2001), Stable isotope composition ($\delta^{18}O$, $\delta^{13}C$) of living planktic foraminifers in the outer Laptev Sea and the Fram Strait, *Mar. Micropaleontol.*, *42*, 163–188.

Watanabe, Y. W., T. Chiba, and T. Tanaka (2011), Recent change in the oceanic uptake rate of anthropogenic carbon in the North Pacific subpolar region determined by using a carbon-13 time series, *J. Geophys. Res.*, *116*, C02006, doi:10.1029/2010JC006199.

Wefer, G., and W. H. Berger (1991), Isotope paleontology: Growth and composition of extant calcareous species, *Mar. Geol.*, *100*, 207–248, doi:10.1016/0025-3227(91)90234-U.

Wierzbowski, H. (2007), Effects of pre-treatments and organic matter on oxygen and carbon isotope analyses of skeletal and inorganic calcium carbonate, *Int. J. Mass Spectrom.*, *268*, 16–29.

Williams, B., J. Halfar, R. S. Steneck, U. G. Wotmann, S. Hetzinger, W. Adey, P. Lebednik, and M. Joachimski (2011), Twentieth century $\delta^{13}C$ variability in surface water dissolved inorganic carbon recorded by coralline algae in the northern North Pacific Ocean and the Bering Sea, *Biogeosciences*, *8*, 165–174.